

Review

Application of Optical Fiber Sensing Technology and Coating Technology in Blood Component Detection and Monitoring

Wenwen Qu ¹, Yanxia Chen ¹, Chaoqun Ma ¹, Donghong Peng ¹, Xuanyao Bai ¹, Jiaxin Zhao ²,
Shuangqiang Liu ^{1,*} and Le Luo ^{1,3,4,5,*}

- ¹ School of Physics and Astronomy, Sun Yat-sen University, Zhuhai 519082, China; quww@mail2.sysu.edu.cn (W.Q.); chenyx687@mail2.sysu.edu.cn (Y.C.); machq3@mail2.sysu.edu.cn (C.M.); pengdh7@mail2.sysu.edu.cn (D.P.); baixy26@mail2.sysu.edu.cn (X.B.)
- ² Center of Cerebrovascular Disease, Zhuhai People's Hospital (Zhuhai Hospital Affiliated with Jinan University), Zhuhai 519600, China; zhaojiaxinhyd@163.com
- ³ Shenzhen Research Institute, Sun Yat-sen University, Nanshan, Shenzhen 518087, China
- ⁴ State Key Laboratory of Optoelectronic Materials and Technologies, Guangzhou Campus, Sun Yat-sen University, Guangzhou 510275, China
- ⁵ International Quantum Academy, Shenzhen 518048, China
- * Correspondence: liushq33@mail.sysu.edu.cn (S.L.); luole5@mail.sysu.edu.cn (L.L.)

Abstract: The advantages of optical fiber sensors include their miniaturization, strong anti-interference ability, high sensitivity, low cost, and fast response speed. They can be used for in situ detection in harsh environments, making them suitable for a wide range of applications such as blood detection and monitoring. This technology holds great potential for medical diagnosis and health monitoring, opening up new possibilities in the field. Coating technology plays a crucial role in enhancing the sensitivity and stability of optical fiber sensors, ultimately improving their measurement accuracy and reliability. This manuscript expounds the application status and progression of optical fiber sensors in the determination of blood glucose concentrations, blood pH, diverse proteins in blood, and physical properties of blood. The principle of optical fiber sensors and the application of coating technology for detecting varying targets are scrutinized in detail, with particular emphasis on the advantages and limitations of distinct design schemes. The adept amalgamation of optical fiber sensing technology and coating technology amplifies the adaptability of optical fiber sensors in diverse practical scenarios, thereby presenting novel instruments and methodologies for researchers in pertinent fields to augment their advancement and development.

Keywords: optical fiber sensors; blood component detection; blood glucose concentration; blood pH; protein in blood



Citation: Qu, W.; Chen, Y.; Ma, C.; Peng, D.; Bai, X.; Zhao, J.; Liu, S.; Luo, L. Application of Optical Fiber Sensing Technology and Coating Technology in Blood Component Detection and Monitoring. *Coatings* **2024**, *14*, 173. <https://doi.org/10.3390/coatings14020173>

Academic Editor: Ihor S. Virt

Received: 21 December 2023

Revised: 25 January 2024

Accepted: 27 January 2024

Published: 30 January 2024



Copyright: © 2024 by the authors. Licensee MDPI, Basel, Switzerland. This article is an open access article distributed under the terms and conditions of the Creative Commons Attribution (CC BY) license (<https://creativecommons.org/licenses/by/4.0/>).

1. Introduction

Optical fiber sensor technology is widely used in the medical field, especially in the detection of various substances and parameters in blood. As a vital part of the fluid environment in the human body, blood carries oxygen, nutrients, hormones, and waste products and reflects important information about the state of human health. Abnormalities in blood vessel wall thickness, blood flow velocity, and parameters like contraction and dilation, or certain substances such as cholesterol and hormones exceeding threshold values, are closely related to conditions such as hypertension, arteriosclerosis, cardiovascular disease, and many other diseases [1,2]. Therefore, the accurate monitoring of various substances and parameters in blood has important clinical and research significance. For example, the continuous monitoring of arterial blood pressure is essential for the treatment and medication adjustment of hypertensive patients [3]. Traditional blood testing methods, which typically require blood samples to be collected and then analyzed in a lab, are not only time-consuming but can also cause discomfort to patients due to wounds. Therefore,

developing a non-invasive, real-time, highly sensitive method for in situ blood testing is an important challenge in the field of medicine. The miniaturization of the fiber sensor makes it possible to monitor one's blood pressure, blood flow rate, and other parameters with high sensitivity in real time, so it becomes a new practical tool for the clinical detection and treatment of diseases. Fiber optic sensors have made remarkable progress in detecting various substances and parameters in blood. For example, they can be used to measure the blood oxygen saturation (S_{pO_2}), blood glucose concentration, blood pH, and concentrations of biochemical molecules such as proteins, hormones, and drugs in the blood [4]. In addition, fiber optic sensors can also monitor one's pulse, blood flow rate, and viscosity in real time [5,6]. It provides clinicians with more comprehensive blood information, which helps in early diagnosis and disease treatment. Fiber optic sensors can be widely used in diagnostics, sensing, and drug management in biomedicine, and their applications are not limited to the above fields and are constantly expanding.

A deep understanding and optimization of the design and coating of fiber optic sensors for blood measurement can improve the accuracy, real-time performance, and patient comfort of the measurement of various parameters in blood. This paper will focus on the current situation and development trend of optical fiber sensing technology and its coating in medical blood detection and analyze the advantages and limitations of different sensor design schemes. In addition, we will discuss the challenges and future directions of fiber optic sensors in blood detection in medicine. The research in this paper can provide more inspiration for the application of optical fiber sensing technology and coating technology in medicine and provide new ideas and possibilities for improving clinical blood detection methods.

2. The Basic Principle of Optical Fiber Sensors

Optical fiber sensing technology began in 1977 [7]; with the rapid development of optical fiber communication technology, optical fiber sensing technology has become one of the standards for measuring the degree of information technology in a country. Optical fiber sensing technology is a sensing technology that uses the optical signal propagating in the optical fiber to perceive the physical quantity to be measured outside. When the temperature, humidity, magnetic field, electric field, and other external physical quantities to be measured change, the characteristic parameters of the light wave transmitted in the optical fiber, such as the phase, light intensity, wavelength, and so on, will change accordingly, and the change relationship between the characteristic parameters and the physical quantity to be measured will be found out so as to inversely derive the change value of the physical quantity to be measured. The schematic diagram of the optical fiber sensing principle is shown in Figure 1. The light emitted by the light source accesses the corresponding sensing region. When the light source remains unchanged, the external physical quantity to be measured will change, which will affect the beam transmitted in the optical fiber through some mechanism, resulting in corresponding changes in the characteristic parameters of the light wave itself. The changed light is received by the optical spectrum analyzer, and the useful signal is demodulated to achieve the purpose of sensing [8,9].

As an emerging sensor technology, fiber sensor technology boasts many advantages, including its high sensitivity, fast response, miniaturization, freedom from electromagnetic interference, suitability for interventional detection, and other characteristics. Therefore, it holds great potential in medical applications.

Based on different sensing principles, optical fiber sensors can be primarily categorized into intensity-modulated sensors, phase-modulated sensors, and wavelength-modulated sensors. Fiber Bragg Grating (FBG) sensors [10] and Surface Plasmon Resonance (SPR) sensors [11] are conventional technologies. FBG combines a Bragg reflector manufactured in a small segment of the fiber core, reflecting a specific wavelength range of the guided mode while transmitting all other guided modes. FBG sensors typically integrate sensitive materials to measure and amplify the sensitivity of the measured parameters. Fixing FBG

in a capillary can achieve temperature sensitivity [12], and utilizing the water accumulation and diffusion characteristics of hydrogels can convert changes in the measured parameters into strain changes in the FBG grating area [13]. SPR sensors are based on surface plasmon resonance in a metal-dielectric waveguide. They measure the refractive index changes caused by the interaction of biological molecules with the SPR sensor surface. The modulation of the refractive index of the analyte medium leads to a resonance wavelength shift. The choice of plasmonic materials for exciting surface plasmons plays a crucial role in the flexibility of manufacturing processes and the performance of SPR-based fiber probes. Silver and gold are preferred plasmonic metals due to their superior optical properties in the visible and near-infrared range.

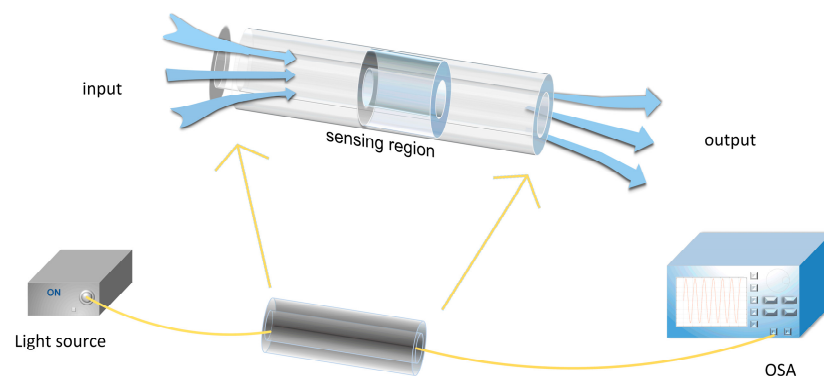


Figure 1. Schematic diagram of the principle of an optical fiber sensor. OSA: optic spectral analyzer.

In addition, Long Period Fiber Grating (LFBG) sensors [14,15], Fabry–Pérot Interferometer (FPI) sensors [16,17], Michelson Interferometer (MI) sensors [18,19], Mach–Zehnder Interferometer (MZI) sensors [20], and others are also mature technologies.

In order to make the optical fiber sensor adapt to various application scenarios and realize the measurement of various physical quantities, the coating layer of the sensor plays an extremely critical role. First of all, the coating layer plays an important role in the protection and durability of the optical fiber sensor; by selecting the appropriate coating material, it can effectively protect the optical fiber sensors from external environment damage such as corrosion, friction, and chemical erosion. This protective coating not only extends the life of the sensor but also ensures reliable operation in harsh conditions [21,22]. Second, through the clever design of the coating layer, the optical fiber sensor can simultaneously detect a variety of target substances, especially to realize the detection of physical quantities or substances that are not sensitive to the optical fiber [23]. The fluorescent optical fiber sensors coated with fluorescent dye can be used to measure a blood glucose concentration with high sensitivity and accuracy. Visible light fiber optic sensors coated with a photosensitive coating can be used to measure S_pO_2 , enabling real-time monitoring of the patient's respiratory and circulatory function. Moreover, the selection of coating materials with specific optical properties can improve the performance of fiber optic sensors such as sensitivity, stability, and response time [24–27]. For example, the fiber sensor coated with anti-protein adsorption coating can reduce the influence of protein adsorption in the blood on the measurement results and improve the measurement accuracy. It should be particularly mentioned that the optical fiber sensor used in medical blood testing can also ensure its biocompatibility through the choice of coating layer to ensure safe and reliable application. The fiber sensor coated with chemical corrosion-resistant coating can resist the corrosion of chemical substances in the blood and prolong the service life of the sensor. In recent years, researchers have focused on improving the selectivity, sensitivity, and stability of fiber optic sensors and have achieved these goals by introducing functional and nanomaterials. However, there are still some challenges, such as long-term stability and feasibility in actual engineering [28–30]. It is worth noting that there is a difference in length between protective coatings and sensing coatings on optical fibers. In contrast to

sensing coatings, the protective coating of optical fibers is typically applied over lengths of several kilometers rather than meters or millimeters. This difference in length indicates that the primary function of the protective coating is to provide protection along the entire length of the optical fiber, while sensing coatings may selectively interact within specific regions of the fiber.

3. Application of Optical Fiber Sensors in Blood Detection

Fiber optic sensors play a key role in blood testing by utilizing optical principles for the sensitive monitoring of blood composition and properties. The sensors using the high sensitivity of the fiber and a fast response time can detect or monitor in real time the physiological indexes in the blood, such as the blood glucose concentration, blood pH value, various protein contents, and other physical characteristics of the blood such as the S_pO_2 .

3.1. Blood Glucose Concentration

Diabetes has become a major health disease, with a rapid increase in the number of patients and high costs worldwide [31]. The continuous monitoring of blood glucose levels is of great significance to guide diagnosis and treatment [32]. Therefore, the development of a simple, compact, fast-response, and high-sensitivity glucose sensor with long-term stability has always been of interest to researchers.

Continuous glucose monitoring (CGM) is commonly employed in outpatient settings to enhance diabetes management. The integration of CGM with insulin injection pumps proves effective in the treatment of diabetes patients [33,34]. Real-time glucose trends are provided by CGM, enabling the detection of abnormal blood glucose levels before clinical symptoms manifest [35]. Biochemical analyzers, utilizing absorbance spectroscopy, serve as the basis and standard for clinically diagnosing diabetes. While these analyzers offer high accuracy, their operation requires skilled professionals and is time-consuming, making them unsuitable for home use by diabetes patients. Home glucose meters, on the other hand, provide rapid and compact testing suitable for community and home use. However, both biochemical analyzers and home glucose meters lack the capability to continuously record dynamic changes in human blood glucose. Consequently, continuous glucose monitoring has emerged as a research focus.

Sensors are the core components of CGM, directly influencing its accuracy. CGM sensors encompass invasive, minimally invasive, and non-invasive categories [36]. Optical technologies have become a global research focus due to their non-invasive, convenient, and safe characteristics. However, challenges such as measurement errors caused by interference from organic substances still need resolution [37,38]. For instance, fluorescence-based glucose sensors exhibit poor long-term stability, and biological molecules similar to glucose may cause interference, leading to false positives [39]. Electrochemical products, the most mature technology with well-commercialized products, have undergone three generations of development for glucose sensors. The first two generations are already mature products in the market, offering high sensitivity. However, their high cost and susceptibility to interference limit their application [40].

Dynamic glucose monitoring involves implanting glucose sensors subcutaneously for the continuous monitoring of glucose concentrations. Clinically, enzymatic electrode sensing technology is utilized for continuous glucose monitoring. However, frequent blood sampling for sensor calibration is typically required. Additionally, enzyme-based sensors struggle to effectively measure low blood glucose levels [41,42]. Fiber optic sensors emerge as promising candidates for glucose sensing due to their advantages of miniaturization, resistance to electromagnetic interference, low cost, and rapid response. Moreover, fiber optic sensors exhibit excellent biocompatibility, making them suitable for in situ detection within the body [43–46].

As early as 1982, Peterson et al. developed a small optical fiber pH probe consisting of two fibers filled with phenol red dye and mounted in a hollow fiber. They proposed that the probe could also be used to measure the glucose concentration [47]. In 1999, a

fiber-based portable system was proposed for detecting and calibrating blood sugar levels using a catheter inserted into a blood vessel; a detector at the end of the catheter captures scattered light and returns it through the fiber to an external computer, which can detect and calibrate blood sugar levels through signal processing [48]. In recent years, due to the rapid development of biology and the emergence of more emerging materials, more types of recognition molecules and coating materials have been combined with optical fiber sensors, which has greatly promoted the improvement of the performance of glucose optical fiber sensors.

In order to realize the real-time monitoring of blood glucose levels in vivo, it is necessary to select a coating material with good biocompatibility.

Graphene oxide (GO), as a branch of graphene research, has the excellent characteristics of a large specific surface area and good biocompatibility, which can form a large number of biomolecular fixed binding sites. Compared with the original graphene material, the functional groups in GO—for example, carboxyl, hydroxyl, and epoxy groups—make it hydrophilic. In addition, GO also has the ability to fix some enzymes, such as glucose oxidase (GOD), etc., which provides a good platform for the further functionalization of the fiber optic sensor [49,50]. In 2018, a tilted fiber Bragg grating (TFBG) glucose sensor based on GO and GOD functionalization was proposed, as shown in Figure 2, which could be used to detect low concentrations of glucose in the range of 0 to 8 mM with a sensitivity of 0.24 nm/mM. The sensitivity of the sensor is 4.5 and 1.7 times higher than that of TFBG without GO layer modification and a glucose biosensor based on LFBG. The method of electrochemical covalent ligase is applied to the optical fiber sensor, which combines the advantages of high sensitivity, in situ measurement, and no labeling of the electrochemical and optical fiber sensors [51]. In 2020, Panda et al. developed a graphene-based prism-coupled SPR biosensor, which deposited a gold layer and GO layer on an N-FK51A prism substrate, which can effectively detect human blood glucose concentrations in the range of 25 to 175 mg/dL. The maximum sensitivity of 271.15°/RIU and the detection accuracy of 1.41°/RIU when the thickness of the gold layer is 55 nm and the number of graphene layers is single-layer are confirmed. This sensor can also be used to detect glucose concentrations in gas analytes and also shows a high sensitivity of 92°/RIU, indicating that this method has potential for development in the field of glucose sensing [52]. In 2023, an extremely-low-detection-limit fiber optic glucose sensor was proposed, which was made by coating the metal surface of TFBG with a GO layer, along with pyrene 1-boric acid (PBA) fixed on the GO layer as a bio-detector. The experimental results show that the sensor has a limit of detection (LOD) of 1 fM and a linear measurement range of 1 fM–10 pM, which can be used to measure the blood glucose concentration in serum and can also be used to measure glucose in tears and sweat due to its low LOD [53].

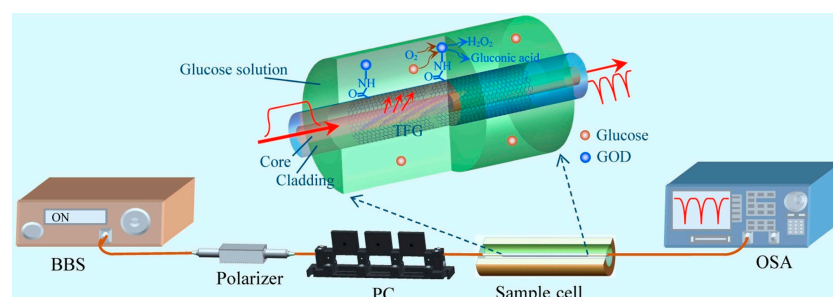


Figure 2. Experimental setup for glucose detection. The upward inset shows the schematical dissection diagram of GOD-GO-modified TFBG. BBS: broadband source; PC: polarization controller [51].

Many chemo mechanical polymers and related hydrogels have also been shown to be useful materials for glucose detection [54–56].

A fiber probe biosensor based on FPI measurement technology can be used to detect pH and glucose. Three pH-sensitive dyes (methyl orange, methyl red, and thymol blue) and three solvent developing dyes (Nile red, rhodamine-B, and 4-amino-n-methylphthalimide)

were mixed with the polymer, respectively. Five pH- and three glucose-sensitive sensing films were obtained and deposited on eight gold nanoparticles coated on a fiber optic probe to obtain five pH and three glucose fiber optic probe sensors. The proposed fiber optic pH and glucose probe sensors have a sensitivity of 1.95 nm/pH and 3.25 nm/mM, respectively, with a high sensing stability and a relative standard deviation of about 2.5%. The proposed sensor provides linear sensing capabilities over a wide range of pH (2–12) and glucose (1 μ M–1 M). The response time and recovery time of the proposed sensor are about 8 s and 9 s, respectively. The sensor has the excellent performance attributes of a fast response, high sensitivity, wide dynamic range, and remote sensing capability, which can be well applied to the field of detection [57]. Alexeev et al. reported a material containing boric acid that facilitates the detection of glucose in tears [58]. In 2023, Li et al. reported a new hydrogel fiber fluorescence sensor functionalized with luciferin derivatives and CdTe QDs/3-(acrylamide) phenylboronic acid (3-APBA). The complex action of the glucose and boric acid group fixed on the hydrogel fiber core will cause local hydrogel expansion. Quantum dots act as signal transducers, which convert hydrogel swelling into fluorescence signal attenuation. The sensor can continuously monitor the dynamic change in a glucose concentration within 0–20 mM. At the same time, since the reaction between PBA and glucose is very sensitive to the pH value, the covalent connection of fluorescein derivatives to the hydrogel fiber core can compensate the pH error in glucose detection and continuously monitor the pH value of 5.4–7.8. The sensor has good biocompatibility and strong anti-interference and can be used for implantation in vivo monitoring. If PBA derivatives with low pKa values (<7) are introduced into the hydrogel fiber, the sensor can also detect glucose under acidic conditions and be used in wearable sensors for sweat glucose detection [59]. The glucose concentration can be measured by etching FBG functionalized with aminophenylboronic acid (APBA) and coated with Reduced Graphene Oxide (RGO) layers. The experimental results show that the sensor coated with the 4-APBA-RGO composite has a more suitable LOD and response range than that coated with 3-APBA-RGO. The etched fiber grating sensor coated with the 4-APBA-RGO composite can detect D-glucose in the concentration range of 1 nM–10 mM, and its LOD is 1 nM. At the same time, the sensor used to detect the hemoglobin concentration in whole blood also showed a low detection limit of 8.6×10^{-5} [60].

The combination of etching technology can enhance the interaction between the evanescent field of the fiber sensor and the surrounding medium so as to improve the performance of the fiber sensor. However, the etching process needs to strictly control the etching environmental conditions and time; otherwise, it is difficult to control the shape of the fiber [61,62]. In 2017, Mohamed et al. made D-shaped SPR-PCF biosensors by etching three rows of photonic crystal fiber (PCF) air holes horizontally, depositing a 50 nm gold layer on the silica surface, and then adding analytes on the gold layer. The sensitivity of the sensor is 200 nm/RIU, and the corresponding resolution is 1.3×10^{-3} RIU⁻¹, but the optical fiber sensor is difficult to make and the mechanical structure is unstable, so it is not conducive to the popularization of use [63]. In 2022, Li et al. proposed a glucose Fiber sensor based on a microsphere Fiber SPR probe. By splicing one end of the single-mode fiber (SMF) with the multi-mode fiber (MMF), the other end was heated by electrode discharge to form a microsphere and plated with gold film. The experimental results show that the sensor has a detection range of 0.1688–200 mg/dL, a maximum glucose concentration sensitivity of 100 nm/(mg/dL), and an LOD of 4 mg/dL. In addition, it is proven that the sensor can resist the interference of sodium ion, potassium ion, sucrose, and chitosan, and the sensor has the advantages of good selectivity and high sensitivity [64]. In 2023, a transmission-type SPR sensor based on unclad fiber was used for glucose detection. The sensor coated a section of step-index multimode fiber with 50 nm Au coating after removing cladding. It is used to measure glucose solutions at concentrations of 0.0001 g/mL and 0.5000 g/mL, with a maximum sensitivity of 161.302 nm/(g/mL) for the lowest glucose concentration and 312.000 nm/(g/mL) for the highest glucose concentration. With a resolution of 0.027 g/mL and good stability, the sensor has great potential for the real-time monitoring of blood

glucose concentrations [65]. Although SPR-based glucose sensors have high sensitivity, they are difficult to be widely used in clinical analysis due to their high cost and poor biocompatibility with heavy metals [66]. Therefore, gold, silver, and other precious metal nanoparticles with a certain biological affinity are often used in biosensors [67]. Using a semipermeable membrane with good biocompatibility as a protection cover is also a desirable method. In 2015, a U-shaped fiber attenuated total reflection (ATR) sensor enhanced by silver nanoparticles used a U-shaped fiber with a bending radius of 2.5 mm, coated with silver nanoparticles and a biological semi-permeable membrane that could pass through glucose as a protective cover. The sensor can be implanted into subcutaneous tissue for continuous glucose concentration detection, and experimental results show that the sensor resolution is 15 mg/mL, about three times that of traditional ATR sensors. Biocompatible semi-permeable membranes have excellent biocompatibility and can allow glucose molecules to pass through while isolating other biomacromolecules [68].

To achieve the real-time monitoring of blood glucose levels in the body, it is also crucial to miniaturize fiber optic sensor products. In 2018, a cone-shaped multi-mode interferometric fiber optic probe modified by GOD was used for glucose sensing. As shown in Figure 3, the fiber is modified by the silanization process, and then GOD is fixed on the MMF through covalent bonding; the probe realized the glucose concentration detection in the range of 0–3.0 mg/mL and realized the accurate detection of glucose content in animal serum samples. The size of this GOD-functionalized fiber optic microprobe glucose sensor was reduced to only a few microns, which is comparable to a single living biological cell. Due to its small size and high sensitivity, it is expected to be applied to the detection of blood sugar in vivo [66]. Combining fiber optic sensors with microfluidic technology to develop high-performance glucose sensors is also a promising solution, as microfluidic technology can provide a miniaturized, low-sample consumption platform for field analysis and detection. In 2016, Yin et al. etched LPFG on a small-diameter single-mode fiber, prepared poly (acrylic acid) (PAA) and poly (ethylenimine) (PEI) multilayer film on its surface through self-assembly technology, and fixed GOD on the multilayer film for glucose concentration detection. The sensor is integrated into a microfluidic chip and can perform the ultra-sensitive detection of glucose solutions with concentrations ranging from 2 μ M to 10 μ M and as low as 1nM, and the response time of the fiber optic sensor is reduced from 6 min to 70 min. This microfluidic chip with integrated fiber optic glucose biosensors has great potential in healthcare and clinical diagnostics [69].

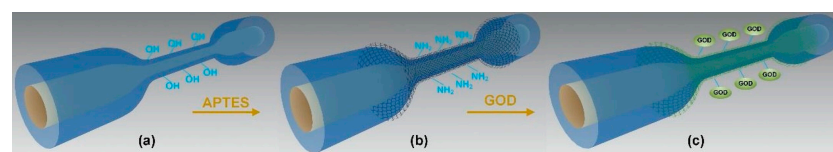


Figure 3. Schematic diagram of GOD immobilization onto a multimode microfiber. (a) Hydroxyl-groups-activated microfiber; (b) APTES-coated microfiber; (c) GOD-immobilized microfiber [66].

The performance comparison of the mentioned fiber optic sensors is presented in Table 1. Due to the narrow bandwidth peak of the FBG spectra, achieving large-range high-resolution demodulation is relatively convenient. Additionally, the implementation of multiple sensors in cascade through wavelength division multiplexing is feasible, making FBG widely applied. However, sensors based on the FBG principle generally suffer from lower sensitivity. In addressing this limitation, researchers often combine etching techniques, utilize TFBG, or apply surface coatings with SPR to enhance sensor performance. Silver and gold are commonly chosen as plasma metals, with gold being the most frequently used in SPR due to its high chemical stability, although silver exhibits poor chemical stability [70]. The preparation of specialty fibers and the use of emerging coating materials play a significant role in improving the performance of glucose fiber optic sensors. This advancement concurrently promotes their direction towards non-invasive and in situ detection. To overcome the drawbacks of glucose sensors based on covalent binding, which

are sensitive to temperature and pH, researchers incorporate compensation sensors for simultaneous multi-parameter measurements. Furthermore, with the rise of wearable technology, attention is directed towards the flexibility and wearability of coating materials, further enhancing the applicability of glucose sensors in the fields of clinical diagnosis and health monitoring.

Table 1. Performance comparison of the above sensing scheme and coating selection.

Sensing Principle	Coatings	Range	Sensitivity	Reference
TFBG	GO and GOD	0~8 mM	0.24 nm/mM	[51]
SPR	Au and GO	25~175 mg/dL	271.15°/RIU	[52]
TFBG-SPR	Au, GO, and PBA	1 fM~10 pM		[53]
FF	Ca alginate	0~20 mM		[59]
FBG	RGO and 4-APBA	1 nM~10 mM		[60]
SPR-PCF	Au	200 nm/RIU		[63]
SPR	Au	0.1688–200 mg/dL	100 nm/(mg/dL)	[64]
Transmission-type SPR	Au	0.0001 g/mL 0.5000 g/mL	161.302 nm/(g/mL) 312.000 nm/(g/mL)	[65]
Multimode interference	GOD	0~3.0 mg/mL		[66]
LPFG	PAA, PEI, and GOD	1 nM~10 μ M (after being integrated into a microfluidic chip)		[69]

3.2. Blood pH

Blood pH analysis is one of the most commonly performed tests for critically ill patients in the operating room and intensive care unit [71]. Dysfunctional pH values can be a typical sign of many deadly diseases, such as cancer and myocardial ischemia [71–74]. In addition, small changes in the pH value can also have a significant impact on nerve activities such as ion regulation and potential changes in nerve cells [75]. Therefore, the high-resolution real-time monitoring of blood pH is necessary. Currently, advanced pH sensors based on colorimetric analysis, fluorescence signals, and electrochemical methods have been proposed [76–78]. Colorimetric or fluorescence-based sensors are given attention due to their ability to provide visual results, but they require professional operators and come with higher costs [73,78,79], making them suitable only for specific occasions. Commonly used electrochemical analyzers have drawbacks such as the need for frequent electrode calibration and susceptibility to electrical interference [80]. Optical fiber sensors can be used as a better solution; they can provide continuous and real-time monitoring, and have many advantages, such as miniaturization and anti-electromagnetic interference, so they have better application prospects in the fields of disease prediction and medical diagnosis [81].

Most pH sensors are based on the use of coating materials with PH-sensitive optical properties, with indicator dyes [82] and hydrogels [83,84] being the most commonly used coating materials for pH sensors. This fluorescence-based fiber-optic sensor (FF) structure, in which a reversible indicator system (colorimetric or fluorescent) is fixed at the fiber end, is attractive because of the large number of indicators that can be used for detection [85–87].

Responding to analytes based on changes in fluorescence intensity is the simplest and most direct method, but the use of intensity changes is unreliable, and the concentration of the analyte may be underestimated or overestimated due to the influence of the illumination source [88]. It is more advantageous to use a fluorescent probe with a wavelength ratio independent of the fluctuation of the light source, and the concentration of the analyte can be confirmed by the ratio of the fluorescence intensity measured at the two excitation or emission wavelengths [89]. In 1976, Peterson et al. developed a fiber optic probe for

the detection of pH in an effort to create an *in vivo* sensor for blood gas analysis and thus proposed the concept of a fiber optic chemical sensor. The sensor probe uses phenol red as a dye indicator, the dye is covalently bound to the polyacrylamide microsphere. Dual-beam spectrophotometry measurement is used because the absorption of red light is independent of the pH value, so it can be used as an optical reference. The green light and red light from the input fiber go from the filler back to another fiber, and its pH value can be calculated based on the measured green light and red light ratio. The accuracy and precision of the sensor are close to 0.01 pH units within the pH range of 7.0 to 7.4. In blood measurement experiments in animals, the results of the fiber optic probe in the first half of the experiment were lower than those of the pH electrode, the pH probe responded faster to pH changes in the second half of the experiment, and there was no similar phenomenon of scaling on the pH electrode after the end of the experiment, so its use time could be extended [90]. In 2018, Wencel et al. reported a rate-based optical pH sensor that physically encapsulated 8-hydroxypyrene 1,3,6-trisulfonic acid (HPTS) into a sol-gel matrix as a pH-sensitive material, deposited on a highly flexible plastic multi-core fiber tip and integrated with electronics for excitation and detection. According to the laboratory results, the pH sensor has a resolution of 0.0013 pH units in the physiological pH range (6.0–8.0) and drifts 0.003 pH units every 22 h. It has the advantages of long-term stability, excellent reversibility, and a short response time (<2 min). The sensor also showed promising performance in *in vitro* whole blood samples and human evaluations conducted under the program, demonstrating the success of the short-term deployment of the sensor *in vivo* [80].

Naphthalimide derivatives were first used for the measurement of blood pH in 2011, and *n*-allyl-4-(4-methylpiperazinyl)-1, 8-naphthalimide was covalently connected to a fluorescence quenching optical pH sensor through thermal polymerization. Experiments in which the sensor measured different concentrations of the buffer solution and rabbit arterial blood showed that the sensor resolution was 0.03 pH units when the pH value was in the range of 6.8–8.0, the correlation coefficient between the pH sensor and the conventional blood gas analyzer was 0.93 *in vivo* ($n = 75$, $p < 0.001$), and the bias and accuracy were -0.02 ± 0.08 pH units. The pH sensor is stable for at least 72 h during the measurement and insensitive to fluctuations in various ion concentrations and plasma permeations at pathophysiological limits, suggesting that it can be used to continuously measure blood pH in a variety of clinical settings [91].

FF has the advantages of a high sensitivity and low detection limit; however, their application is limited due to the photobleaching of fluorophores in practical applications [92,93]. Many sensors are not originally developed for use in the human body, but with the advent of more suitable optical fibers, optoelectronic components, and emerging coating materials, the sensing layer can be modified or optimized for use in human detection [94]. Therefore, the sensor design with a dynamic detection range including a normal human blood pH range and good biocompatibility of the coating material has great potential for application in human blood detection. Ionic hydrogels are stimulus-responsive gels that can reversibly swell/deswell in response to changes in surrounding conditions. Among various ionic hydrogels, polyacrylic acid (PAA) is widely used because of its biocompatibility [95–97], water absorption, and good film formability [98]. Ultra-sensitive pH sensors can be developed by printing PAA ionic hydrogels with high accuracy on the surface of tapered LPFG optical fibers with a diameter of 30 μm . With a sensitivity of 7.5 nm/pH in the pH range of 2 to 7, a resolution of about 0.0027 pH units, and a rapid response, the micropatterning method demonstrated by the sensor will trigger innovation in PAA ionic hydrogels for sensing applications [99].

Smart hydrogels are also one of the popular coating materials for pH monitoring [100,101]. A smart hydrogel composed mainly of acrylamide, bisacrylamide solution, and methacrylic acid coated on LPFG can be used for pH detection. Sealed in a flow cell with a known pH solution, the sensor shows an ultra-high average sensitivity of 0.66 nm/pH and a response time of less than 2 s over a pH range of 2 to 12, enabling almost a full range of pH

measurements [102]. In 2018, Zhao et al. proposed a hydrogel-coated SPR sensor based on an MMF-SMF-MMF structure for pH measurement, as shown in Figure 4. The sensor is coated with a silver film on the surface of the SMF fiber and a smart hydrogel coating composed mainly of acrylamide (AAM), N, N'-methylene diacrylamide (BAAM), N,N,N,N-tetramethylethylenediamine (TEMED), and methacrylic acid. Experiments have shown that it can monitor a wide range of pH values from 1 to 12. The sensitivity is 13 nm/pH in the pH range of 8 to 10. The experiment also proves that the hydrogel layer can improve the sensing performance of an SPR sensor and protect the silver film at the same time [103].

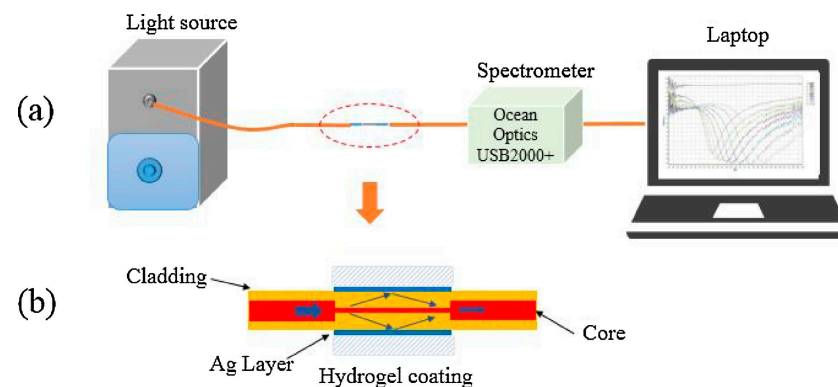


Figure 4. (a) Experimental setup of the sensing system; (b) Schematic of the hydrogel-coating optical fiber SPR sensing part [103].

In recent years, the development of pH sensors with good biocompatibility, good stability, and rapid responses has become more and more popular research, and more and more coating materials have been developed for pH detection. The easily synthesized polyaniline (PANI) has excellent biocompatibility, stability [104], and fast reversible adsorption and desorption kinetics. In 2015, Chiam et al. used FBG-based sensors to study the influence of the doping ratio on the pH detection performance of PANi-coated Fiber Bragg Grating [105]. In 2018, a pH sensor that deposited PANi on the surface of TFBG by in situ chemical oxidation was proposed. Experiments show that the sensitivity of the sensor is directly related to the thickness of the coating film. The thickness of the film is less than 2 μm , which will lead to large areas of TFBG not being covered. With the increase in the thickness of the film, the hysteresis phenomenon will also increase. The sensor has an overall sensitivity of 46 pm/pH units in the pH range of 2 to 12, and the combination of the sensor characteristics means that it can also be used in other fields, such as medical smart textiles [106], bioelectricity, and in vivo measurement [101,107,108]. In 2021, Wang et al. proposed a pH biosensor based on DNA-functionalized microfiber-assisted MZI, as shown in Figure 5. By combining the i-motif as a Ph-sensitive nucleic acid with its complementary sequence, the complementary DNA enhancement mechanism can be utilized to improve pH sensitivity as well as counter matrix effects caused by the influence of the volume refractive index of pH sample liquid. The experimental results show that the pH value detection range of the MZI sensor is 4.98–7.4, the maximum sensitivity is 480 pm/pH, and the resolution is 0.042 pH units. This complementary DNA-enhanced fiber optic sensor is expected to enable biocompatible, marker-free, and highly sensitive pH sensing. In addition, it paves a new way for the development of novel DNA nanomachine-assisted fiber optic sensors [109].

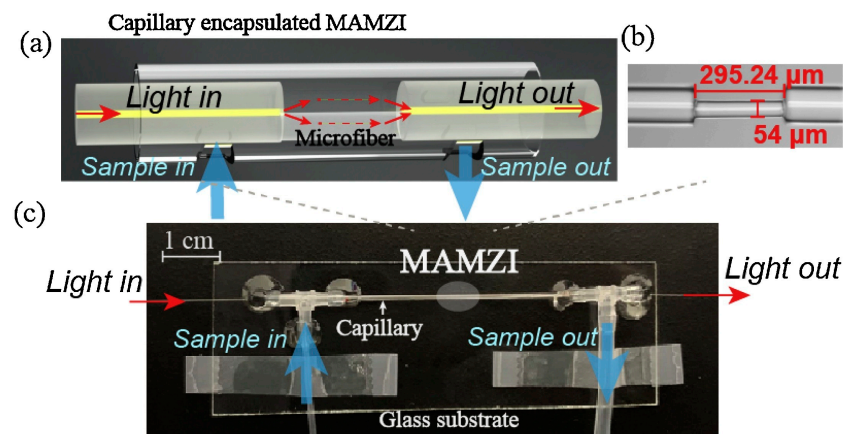


Figure 5. (a) Schematic diagram of the proposed MAMZI structure; (b) Microscopic image of the fabricated MAMZI; (c) Photograph of the encapsulated microfluidic chip [109].

The acid-base balance in the human body is regulated by multiple organs and systems in the body, so changes in pH also affect multiple organs at the same time [110]. In addition to the monitoring of human pH values in the blood, the real-time monitoring of cerebrospinal fluid [110,111], intestinal fluid, and intracellular fluid [112] is also of great guiding significance for medical diagnosis. In 2023, Zhou et al. proposed a hydrogel-coated fiber pH probe based on fluorescence ratio detection, which connected PH-sensitive fluorescent microspheres to one end of MMF coated with PEGDA hydrogel. Experiments in rodent brains show that the probe has a pH detection range of 3.0~9.0 and a resolution of 0.0014 pH units in a pH range of 7.0–8.0. This biocompatible hydrogel-coated fiber probe provides a unique solution for assessing small changes in the pH of the brain microenvironment [113]. In 2021, Podrazky et al. used a fiber optic sensor to measure the pH value of human aqueous humor samples during cataract surgery. The sensor was constructed by fixing HPTS as a fluorescent dye in a mixed sol-gel matrix at the tip of a conical fiber and measured the samples using the fluorescence ratio. The experimental results showed that its accuracy and response time were comparable to those of standard pH electrodes [94].

Comparing the work presented in this paper with the performance of previously reported laboratory-based and commercially available pH sensors, as shown in Table 2, it is clear that the limitations encountered by current fiber-optic sensors for blood pH detection are not due to sensor performance but to scaling, long-term stability, biocompatibility, and calibration limitations for use in real-world scenarios [114]. Therefore, in addition to paying attention to the improvement of the sensor's own performance, it is more important to consider how to put excellent sensing solutions into large-scale manufacturing and use. For pH monitoring in the human body, the biocompatibility and stability of the sensor need to be further optimized, especially in real-time monitoring in the human body, and the requirements for coating materials are more stringent. Second, with the development of internet of things and telemedicine monitoring, future fiber optic pH sensor coating materials may integrate advanced communication technologies to achieve real-time monitoring and transmit data to remote locations, enabling users to access body pH data anytime, anywhere.

Table 2. Performance comparison of the above sensors with previous laboratory and commercially available blood pH sensors.

Sensing Principle	Coatings	Range	Resolution/pH Units	Reference
Ratiometric fluorescence signal	HPTS	6.0~8.0	0.0013	[80]
Ratiometric fluorescence signal		6.0~8.0	0.03	[91]
LPFG	PAA ionic hydrogels	2~7	0.0027	[99]
LPFG	Smart hydrogels	2~12		[102]
SPR	Smart hydrogels and Ag	1~12		[103]
TFBG	PAni	2~12		[101]
MZI	DNA(i-motif)	4.98~7.4	0.042	[109]
Lesonco pH sensor (Commercial)		0.00~14.00	0.01	[115]
G-PHT1 pH tester (laboratory)		0.00~14.00	0.1	[116]
Presens pH sensor (Commercial)		5.5~8.5	0.01	[117]
Analog pH sensor (Commercial)		0~14	0.01	[118]

3.3. Protein in Blood

When a pathogen or other foreign protein (antigen) invades an animal, the body produces antibodies that recognize these foreign objects and remove them from the body. The antigen and antibody combine to produce an immune reaction, which has high selectivity and sensitivity [119]. The immune sensor is a biosensor developed by using the recognition function of the antigen (antibody) to the antibody (antigen). The immune sensor is composed of a photosensitive element as an information converter and a biometric molecule fixed on the sensor. The use of different biometric molecules generates a changing optical signal through its interaction with the light of the optical element, and the immune response can be detected by detecting the changing optical signal.

Proteinuria is used to describe a patient with the excessive excretion of protein in urine, defined as more than 300 mg of protein excreted per 24 h, which precedes any detectable decline in renal filtration function [120–122]; the protein content in human urine usually does not exceed 150 mg/24 h, which is difficult to identify by conventional detection methods. In 2016, a TFBG sensor with a plasma nanocoating was proposed for detecting changes in urine proteins. The biosensor is coated with silver nanomaterials on commercially available single-mode fibers engraved with TFBG, and by reducing the silver film thickness to about 20–30 nm instead of 50 nm for optimal SPR excitation, different modes of TFBG spectra show very high but opposite sensitivities to RI changes around TFBG. Using this device, different concentrations of protein in rat urine can be clearly distinguished between healthy samples, kidney samples, and treated individual samples, with a protein concentration sensitivity of 5.5 dB/(mg/mL) and an LOD of 1.5×10^{-3} mg/mL. These results show a clear relationship between protein efflux and changes in the urine sample RI between 1.3400 and 1.3408, pointing the way for the evaluation and development of new drugs for the treatment of kidney disease. On the one hand, the integration of TFBG with microfluidic channels allows for the precise measurement control of samples with sub-microliter volumes, and since the inherent temperature cross-sensitivity of TFBG devices is eliminated,

precise temperature control is not required. On the other hand, the integration of TFBG with a hypodermic needle will allow similar measurements to be made *in vivo* [123].

Glycoproteins have been shown by researchers to be involved in a variety of diseases, including diabetes and neurodegenerative diseases [124], and when glycoproteins on the surface of cells enter the blood circulation, they can become special signals that provide important information [125]. In 2017, a TFBG-SPR unlabeled glycoprotein sensor with a boric acid derivative (ABA-PBA) as a receptor molecule achieved a high sensitivity and selectivity for glycoprotein detection. Using boric acid derivatives as the biometric molecules of the sensor, the material is widely used as the recognition substrate of biolecular-containing diol. TFBG can improve the quality factor by two orders of magnitude, so the combination of boric acid and the TFBG sensor is beneficial to detecting different glycoproteins. The interaction between boric acid and glycoprotein works well in an alkaline environment ($\text{pH} > 8.5$). However, bioassays usually require a neutral environment. To solve this problem, the team synthesized a phenylborate tertiary amine derivative, giving the sensor a pH of about 7. The sensitivity of the sensor to the protein concentration can reach $2.867 \text{ dB}/(\text{mg}/\text{mL})$, the LOD is $2 \times 10^{-5} \text{ g}/\text{mL}$, and it has good repeatability [126].

Myoglobin (Mb) is an oxygen-binding heme protein mainly distributed in cardiac muscle and skeletal muscle tissue. In acute myocardial injury, Mb is the first to be released into the blood, so Mb measurement helps to detect the presence of reinfarction during the course of acute myocardial infarction [127]. In 2017, Tomyshev et al. designed a fiber optic plasmon refractive index sensor. In order to improve the stability of the sensor, different from other sensors based on TFBG and SPR, it is commonly used to measure the transmission spectrum of the optical signal propagated through the sensor and then transmitted to the receiving device. The sensor is coated with a reflective film at the end of one section of the optical fiber to detect the reflected signal. This structure allows for avoiding the second mounting point of the sensor and making the optical fiber in a free position. Due to this characteristic, the impact of vibration and mechanical stress on sensor operation is significantly reduced. Further experiments show that this decision improves the stability of the sensor data at rest by at least one order of magnitude, and the sensor exhibits both high sensitivity and high resolution, with a resolution of about $2 \times 10^{-6} \text{ RIU}$ in an aqueous solution, which is almost an order of magnitude better than previously published results. The sensor reliably detects low concentrations of proteins in the solution, successfully detecting myoglobin at a concentration of $500 \text{ ng}/\text{mL}$ in acetate buffers [128].

Protein aggregation, misfolding, and the like that typically occurs in neurodegenerative diseases can have damaging effects on cellular processes [129,130] and are associated with aging [131]—for example, Alzheimer's Disease (AD), which is characterized by the aggregation of β -amyloid and Tau proteins [132,133], or Parkinson's disease, where α -synuclein aggregation occurs [130]. The biosensor based on the FPI end resonator can effectively detect the concentration of protein aggregates in a simple and quick manner. The protein aggregation level in bovine serum albumin protein preparation is characterized by the biosensor. The experimental results obtained are consistent with the results of commonly used fluorescence level analysis detection technology, which proves the applicability and effectiveness of the sensor. The development of the probe can be used as a non-invasive device for the diagnosis of degenerative diseases and drug production. In addition, the sensor probe geometry with different cavities that are simultaneously actuated can be used for multi-parameter monitoring, which will modulate the cavity of the resonator probe more significantly [134]. At the same time, because neurodegenerative diseases are persistent and progressive, it is necessary to take effective measures for the early diagnosis of AD before the lesions become too severe to be cured. In 2018, an SPR fiber sensor for the immunoassay of tau proteins (total tau protein and phosphorylated tau protein) in human serum was proposed. The sensor removed 5 cm of cladding along the length of the multimode fiber and produced an asymmetric coating of 1 nm-thick Cr and 40 nm-thick Au on the exposed fiber core surface by a hot evaporator, as shown in Figure 6. The uneven contour of the coated metal can support more fiber modes to stimulate SPR,

which is conducive to improving the sensitivity of the sensor. The test results showed that the LODs of the total tau protein and phosphorylated tau protein were 2.4 $\mu\text{g}/\text{mL}$ and 1.6 $\mu\text{g}/\text{mL}$, respectively. Comparing the measured results with the results of the ELISA kit, it was found that the SPR fiber sensor measurements produced heterogeneity in the average concentration of the total tau protein and phosphorylated tau protein increased relative to the control of AD patients. This was attributed to the difference in affinity strength between the antibodies used in the ELISA kit against the two types of tau protein and the antibodies used in the SPR fiber sensor. According to this heterogeneity, it can be speculated that the serum of AD patients is more likely to produce unphosphorylated tau protein, which is considered to be one of the potential key factors that play an important role in the progression of AD [135].

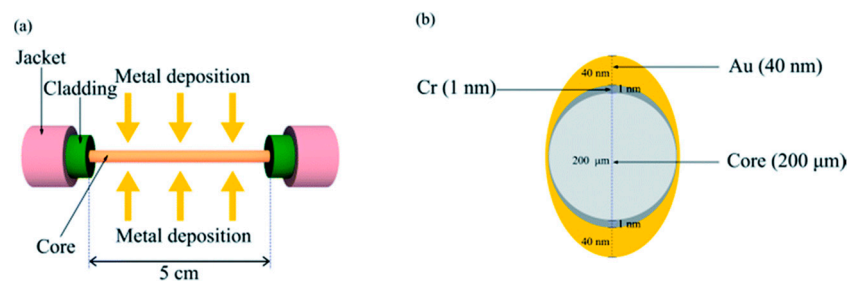


Figure 6. (a) Cr/Au coating on a fiber core; (b) Asymmetric cross-section of metal layers coated on the fiber core [135].

Immunoglobulin G (IgG) and IgG subclasses have always been associated with chronic infections, and the growing awareness that defects or increases in selected IgG subclasses may have clinical consequences has led to a strong interest in quantifying the IgG isotype [136,137]. In 2019, Wang et al. first proposed and demonstrated a highly sensitive TFBG-SPR biosensor based on GO and Staphylococcal Protein A (SPA) co-modification for IgG detection. The gold film on the surface of the sensor was first fixed with GO and then modified with SPA to improve the sensitivity of the sensor. Experimental results showed that the sensitivity and LOD of the GO-SPA modified TFBG-SPR biosensor were about 0.096 dB/ $(\mu\text{g}/\text{mL})$ and 0.5 $\mu\text{g}/\text{mL}$. It showed a better response to human IgG concentrations in the range of 30–100 $\mu\text{g}/\text{mL}$ than the TFBG-SPR sensor modified with GO or SPA alone. Its sensitivity is 2.40 times higher than that of an SPA-modified TFBG-SPR biosensor and 1.78 times higher than that of a Go-modified TFBG-SPR biosensor, respectively. At the same time, the sensor has the advantages of an excellent stability, high precision, and flexible production [138]. The optical fiber biosensor platform based on high-reflectivity FBG also provides a competitive optical fiber platform for targeted biomolecular detection. The schematic diagram of FBG composed of high-reflection FBG, graded refractive index MMF, and SMF is shown in Figure 7. The experiment of detecting IgG in serum by this sensor has verified the specificity of the FBG sensor. At the same time, the sensor achieved an ultra-low detection limit of 32 pM by coating the sensing surface with GO and anti-IgG functionalization without using the signal amplification of functionalized gold nanoparticles or second antibodies. It has great application potential in labeling free biosensing [139].

Dengue fever is a dengue virus (DENV) infection transmitted to humans through the bite of infected mosquitoes, Dengue virus is divided into four serotypes, I, II, III, and IV, and each type has the ability to infect and cause disease. According to the World Health Organization 2023, about half of the world's population is currently at risk of dengue fever, with an estimated 100 million to 400 million people infected each year. In 2019, Kamil et al. reported a functionalized cone-fiber biosensor with a deposited GO layer for the detection of DENV II E protein. The conical area was deposited with GO and functionalized with anti-DENV II E protein IgG antibodies for testing at different concentrations of DENV II E protein. The test results of different GO layer thicknesses show that when the GO layer thickness is 16.17 nm, the optimal sensitivity value of the sensor is 12.77 nm/nM, and the

LOD is 1 pM. The sensor shows a high accuracy, selectivity, and affinity in tests. The sensor undoubtedly demonstrates the great potential of nanomaterials' integration in the field of dengue diagnostics [140].

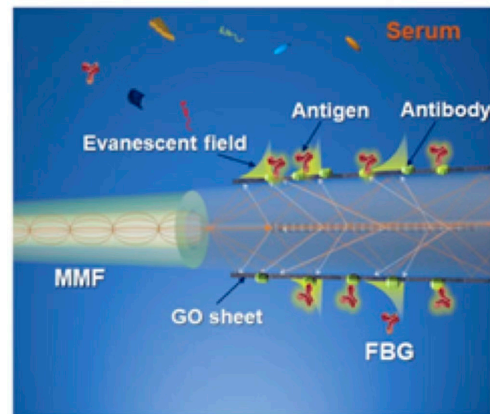


Figure 7. The schematic overview of the FBG sensor [139].

Cardiac troponin I (cTnI) is considered to be the most obvious and direct indicator of Myocardial injury [141,142] and has been established as the gold standard for detecting Acute Myocardial Infarction (AMI). Therefore, it is necessary to develop a labeling-free, simpler, and more efficient detection method [143]. A Local Surface Plasmon Resonance (LSPR)-based heterocellular fiber sensor structure can be used to detect cTnI. By etching the SMF-MMF-SMF (SMS) structure and then fixing gold nanoparticles (AuNPs) and cerium oxide nanoparticles (CeO_2 -NPs) on the fiber structure, the performance and stability of this sensor probe were improved while ensuring its biocompatibility. The LOD and sensitivity of the sensor are 108.15 ng/mL and 3 pm/(ng/mL), respectively, and the sensor has good repeatability and stability in the range of normal human serum pH values. Due to the advantages of easy manufacture, high sensitivity, a wide linear range, and the ability to detect the whole range of human cardiac troponin concentrations, it is suitable for the diagnosis of AMI [144].

The above review covers the application of immunosensors in the detection of urinary proteins, glycoproteins, myoglobin, neurodegenerative disease markers, and immunoglobulins. These studies demonstrate the broad use of fiber-optic immunosensors in the biomedical field, providing new tools and methods for the early diagnosis and treatment of diseases. The performance and reliability of optical fiber immune sensors largely depend on their coating material; the selection of highly selective and highly sensitive materials is necessary in order to increase the sensitivity of the sensor, which can adopt more nanomaterials to enhance the number of material sensing molecules, while in order to achieve the remote and real-time monitoring of optical fiber immune sensors, it is also necessary to choose better biocompatible coating materials, which are critical to understanding complex biological processes and disease mechanisms in living organisms.

3.4. Blood Physical Characteristics

The cardiovascular system is a closed transport system made up of the heart, blood vessels, and blood, and many hormones and other information substances also reach their target organs through blood transport to adjust body functions. Healthy and fully functional vasculature plays an important role in delivering nutrients to cells and protecting organs. Therefore, realizing the non-invasive real-time detection of vascular dysfunction is of great significance in biomedical research [145].

The term “blood flow” has been used to refer to different quantities such as the volumetric blood flow or the maximum velocity of red blood cells in a volume, and intravascular flow measurements can be used to assess abnormalities in the shape of blood vessels in the brain [146,147]. Positron emission tomography (PET) is often quantified as

the “gold standard” technique for blood flow measurement, but its use in specific scenarios is limited due to its long scan time for acute patients [148]. Ruiz-Vargas et al. demonstrated a method for measuring instantaneous changes in flow during pulsating blood flow using a flow sensor consisting of an FBG sensor and a 565 nm light-emitting diode, LED lighting to heat the blood, and a fiber-optic sensor to detect temperature fluctuations due to flow changes. Experiments show that the Pearson coefficient between the results obtained by this method and the results obtained by an ultrasonic signal ranges from -0.83 to -0.98 , and the coefficient depends on the pulsation frequency when the pulsation blood flow rate is 20–900 mL/min. This method allows for intravascular blood flow measurements under pulsatile flow conditions, presenting potential applications in medical settings requiring continuous blood flow sensing. However, further research is needed to determine the sensor’s behavior under various physiological conditions and to examine different configurations to ensure human safety [149]. In 1975, it became possible to perform invasive blood flow velocity measurements in rabbits using a single-fiber catheter with a diameter of 0.5 mm [150]. The existing methods of blood flow velocity measurement include ultrasonic Doppler detection, laser Doppler detection, and blood flow velocity measurement between two points [151]; compared with other methods, the combination of the laser Doppler method and optical fiber has a higher resolution. In 1983, Tahmoush et al. developed a semi-invasive disk sensor for measuring the blood flow velocity in muscle. The disk surface exposes the ends of two tightly connected optical fibers to the tissue, which can be placed on the biopsied exposed muscle surface for detection [152]. Laser Doppler velocimeters have moved in the direction of non-invasive measurement. Laser Doppler methods have been used for the noninvasive detection of blood flow in situations where light can be transmitted through the vessel wall [153]. However, the laser Doppler method mainly measures the movement rate of red blood cells, rather than the whole blood flow velocity, so spatial variations may cause spatial deviations in blood flow estimates [154].

S_pO_2 is the percentage of the volume of oxygenated hemoglobin bound by oxygen in the blood to the total volume of hemoglobin bound, which is the concentration of blood oxygen in the blood. In normal people, the S_pO_2 of arterial blood is 98%, and that of venous blood is 75%. Monitoring the S_pO_2 of arterial blood can estimate the oxygenation and hemoglobin oxygen-carrying capacity of the lungs, and thus, the effectiveness of the cardiopulmonary system can be evaluated [153]. Continuous oxygen saturation measurement is also valuable in patients with respiratory failure who are undergoing extracorporeal carbon dioxide removal therapy [155]. Currently, the predominant method for measuring S_pO_2 is based on photoplethysmography (PPG) [156]. To accurately calculate S_pO_2 , the average of multiple pulse cycles is required to enhance precision, resulting in a loss of real-time measurement [157]. In 2018, Liu et al. proposed a novel integrated optical fiber sensor probe that combines contact pressure for detecting S_pO_2 . Figure 8 shows the probe design. The sensor comprises three plastic optical fibers (POF) and one FBG sensor. Each plastic optical fiber used in the pulse oximeter is split at a 45° angle at its distal end. All fibers are encapsulated in a biocompatible epoxy resin patch to reduce motion artifacts in the photoplethysmogram (PPG). Additionally, this design allows for the conversion of lateral loads into the axial strain in the FBG. Test results indicate that combining pressure measurements from FBG and a reference FBG yields reliable results with lower latency and relatively minimal temperature influence. The measurement error for contact force within the range of 5 to 15 kPa is less than 2%. In wearable technology, this probe could be employed to optimize the fit of garments utilizing this technology, achieving reliable measurement results by applying appropriate pressure. A reference FBG for temperature compensation has been added to the sensor, and in future designs, a compensation FBG for the axial strain could be incorporated to eliminate axial strain interference. Additionally, algorithm modifications for calculating S_pO_2 could be implemented to reduce discrepancies between the designed sensor and commercial pulse oximeters [158].

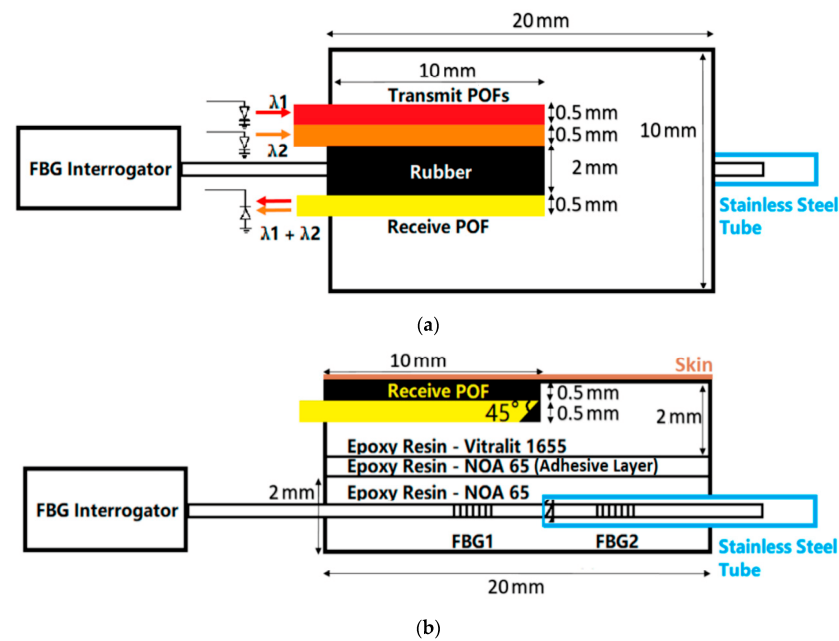


Figure 8. (a) Plan view of the probe; (b) Side view of the probe [158].

Pulse waveform analysis (PWA) was a commonly used and effective diagnostic tool from routine clinical examination to disease diagnosis. The radial pulse waveform was a predictor of radial coronary artery diagnosis [159–161], and vital signs such as arterial stiffness and cardiovascular status could be estimated by digital conversion to the central column arterial pressure [162–164]. It has been proven that the use of FBG sensors made of POF can solve the problem of quartz fiber easily breaking and forming sharp edges. The experimental results show that the pulse wave signal can be measured by the POF-FBG sensor, and its signal-to-noise ratio (SNR) is at least eight times higher than that of quartz FBG. The obtained pulse wave signal is processed and the calibration curve is constructed by the least square method. The blood pressure calculated by the least square method has a low error. However, the correlation between POF-FBG and accelerated plethysmograph (APG) was 0.54–0.72, which did not meet the author's expectation. In addition, experiments have shown that pulse wave signal measurements reflecting pulse wave signals should be considered to improve the accuracy of blood pressure measurements, while reference blood pressure measurements over a large range are needed in subsequent experiments to improve the correlation coefficient of the calibration curve [165]. In 2020, Pant et al. developed and demonstrated a novel, non-invasive Fiber Bragg Grating Plethysmographic pulse recorder (FBGPPR). The device consists of a silicone diaphragm attached to a hollow plastic conical tube, which binds the FBG sensor laterally to the silicon diaphragm. When the device is worn on the finger of the subject, the developed FBGPPR captures the volume change in the blood in the form of a pulse waveform, and the collected pulse waveform is analyzed to obtain the APG. The experimental results are consistent with the previously reported acceptable range for this age group, so the device can effectively acquire the pulse pressure waveform. In addition, arterial pulse waveforms can be collected from the developed FBGPPR with an electronic stethoscope to assess the pulse transit time (PTT); PTT is a measure of pulse wave velocity and arterial stiffness, which can indicate a person's cardiovascular status. Obtaining PTT can help to further estimate important cardiovascular parameters, such as the arterial flow velocity and arterial stiffness index, and is also an indirect method for estimating blood pressure [127,166]. Traditional Chinese medicine (including pulse theory) has been used clinically for thousands of years, in which the detection of the radial pulse waveform at different locations on the wrist is one of its necessary indicators [167–169]. So far, the measurement of the radial pulse waveform in traditional Chinese medicine is still mainly based on the doctor's experience [170]. Therefore,

accurate measurement can also provide a good platform for the scientific understanding and research of Chinese medicine. A novel optical measurement system based on FBG and a lever amplification mechanism can also be applied to high-sensitivity radial artery pulse waveform measurements. The device utilizes a controlled carbon fiber tube to form a lever, amplifying the force F_2 generated by periodic pulses to F_1 before applying it to the FBG. Experiments demonstrated that the sensitivity of the proposed sensor increases with an increase in the lever arm ratio. When the ratio is 6.2, the sensitivity of the FBG sensor reaches 8.236 nm/N. Compared to previous works, this FBG sensor exhibits higher sensitivity and a better SNR, making it more suitable for capturing details in pulse waveforms. Due to the similarity between the results obtained by the FBG sensor and the pulse waveforms measured by an electrical pulse measurement system, this sensor demonstrates good applicability. Furthermore, this sensor can detect waveforms at multiple positions and depths, providing a measurement platform for medical communities, including traditional Chinese medicine. However, the sensor has limitations that need optimization. First, the inclusion of a limiter to protect the FBG from external force may restrict the sensor's sensitivity improvement. Therefore, alternative encapsulation methods should be considered to ensure FBG stability. Second, considering the sensitivity of FBG to temperature, the practical use of the sensor requires the addition of a temperature-compensating FBG to eliminate temperature interference. Lastly, as motion artifacts can impact the accuracy of detected waveforms, it is essential for patients to remain still during measurements [171].

In addition to the above-mentioned fiber optic sensors used for blood flow, flow velocity, S_pO_2 , PWA, and other fields of monitoring, fiber optic sensors have also made progress in the monitoring of other physical characteristics of blood, such as blood viscosity [172], thrombosis detection [173], etc. In the future, the application of fiber optic sensors will continue to develop in the direction of more comprehensive blood detection.

4. Conclusions and Prospects

Optic fiber sensors have gained widespread application in the medical field due to their unique capabilities. With continuous technological advancements, their use in blood detection and monitoring is expected to become even more extensive. In the future, the applicability of sensors in medical diagnostics and healthcare will be strengthened through the process of selecting sensing and coating technologies and implementing sensing solutions in practical use. In the selection of sensing and coating technologies, fiber optic sensors may integrate with advanced technologies such as artificial intelligence and big data, enabling more efficient and precise blood detection and monitoring. Additionally, with the development of biocompatible materials, fiber optic sensors may find applications in implantable monitoring devices within the human body, facilitating the long-term and continuous monitoring of physiological parameters.

In the manufacturing of fiber optic sensors, improvements in design, manufacturing processes, and coating material selection can enhance their accuracy and sensitivity. This can enable the better detection and monitoring of biomolecules and parameters in the blood, allowing for simultaneous multi-parameter detection and providing more comprehensive physiological information for the medical and healthcare field. Concurrently, advancements in biomedical engineering and medical imaging technologies may see fiber optic sensors combined with techniques like endoscopy and optical coherence imaging, offering doctors more intuitive and in-depth insights into medical conditions.

The implementation of superior sensing solutions on a large scale requires considerations for miniaturization and portability in the design of fiber optic sensors. This would make them suitable for diverse applications, including home monitoring and mobile healthcare. In summary, the future outlook for the application of fiber optic sensors in blood detection and monitoring is promising, promising revolutionary advancements in the medical and healthcare domain. With technological progress, we anticipate that fiber optic sensors will play a more significant role in the medical field, safeguarding our health.

Author Contributions: Conceptualization, S.L. and J.Z.; methodology, W.Q. and J.Z.; formal analysis, Y.C.; investigation, C.M.; resources, D.P.; data curation, X.B.; writing—original draft preparation, W.Q.; writing—review and editing, S.L. and L.L.; supervision, S.L. and L.L. All authors have read and agreed to the published version of the manuscript.

Funding: National Key Research and Development Program (Grant No. 2022YFC2204402), Guangdong Science and Technology Project (Grant No. 20220505020011), Shenzhen Science and Technology Program (Grant No. 2021Szvup172), and Shenzhen Science and Technology Program (Grant No. JCYJ20220818102003006).

Institutional Review Board Statement: Not applicable.

Informed Consent Statement: Not applicable.

Data Availability Statement: Data-sharing is not applicable to this article.

Conflicts of Interest: The authors declare no conflicts of interest.

References

1. Li, Q.; Ding, L.Y.; Zhang, Y.M.; Wu, T. A Cholesterol Optical Fiber Sensor Based on CQDs-COD/CA Composite. *IEEE Sens. J.* **2022**, *22*, 6247–6255. [[CrossRef](#)]
2. Fasseaux, H.; Loyez, M.; Caucheteur, C. Plasmonic optical fiber for insulin detection through phase analysis. In Proceedings of the European Workshop on Optical Fibre Sensors (EWOFS 2023), Mons, Belgium, 23–26 May 2023; p. 1264311. [[CrossRef](#)]
3. Parati, G.; Ochoa, J.E.; Lombardi, C.; Bilo, G. Blood Pressure Variability: Assessment, Predictive Value, and Potential as a Therapeutic Target. *Curr. Hypertens. Rep.* **2015**, *17*, 23. [[CrossRef](#)]
4. Perez, J.L.C.; Gutiérrez-Gutiérrez, J.; Mayoral, C.P.; Pérez-Campos, E.L.; Canseco, M.D.P.; Carrillo, L.T.; Mayoral, L.P.C.; Treviño, M.V.; Apreza, E.L.; Laguna, R.R. Fiber Optic Sensors: A Review for Glucose Measurement. *Biosensors* **2021**, *11*, 61. [[CrossRef](#)]
5. Legendre, J.P.; Forester, G.V. A fibre optic sensor of physiological parameters. *Proc. SPIE-Int. Soc. Opt. Eng.* **1986**, *661*, 218–223. [[CrossRef](#)]
6. Kokkinos, D.; Dehipawala, S.; Holden, T.; Cheung, E.; Musa, M.; Tremberger, G.; Schneider, P.; Lieberman, D.; Cheung, T. Fiber optic based heart-rate and pulse pressure shape monitor. In Proceedings of the Conference on Optical Fibers and Sensors for Medical Diagnostics and Treatment Applications XII, San Francisco, CA, USA, 21–22 January 2012.
7. Starodumov, A.N.; Zenteno, L.A.; Monzon, D.; de la Rose, E. Fiber Sagnac interferometer temperature sensor. *Appl. Phys. Lett.* **1997**, *70*, 19–21. [[CrossRef](#)]
8. Chen, J.; Liu, Q.; He, Z. Time-domain multiplexed high resolution fiber optics strain sensor system based on temporal response of fiber Fabry-Perot interferometers. *Opt. Express* **2017**, *25*, 21914–21925. [[CrossRef](#)] [[PubMed](#)]
9. Tian, Z.; Yam, S.S.H.; Loock, H.-P. Single-mode fiber refractive index sensor based on core-offset attenuators. *IEEE Photonics Technol. Lett.* **2008**, *20*, 1387–1389. [[CrossRef](#)]
10. Fan, Z.; Diao, X.; Hu, K.; Zhang, Y.; Huang, Z.; Kang, Y.; Yan, H. Structural health monitoring of metal-to-glass-ceramics penetration during thermal cycling aging using femto-laser inscribed FBG sensors. *Sci. Rep.* **2020**, *10*, 12330. [[CrossRef](#)] [[PubMed](#)]
11. Zhao, Y.; Tong, R.-J.; Xia, F.; Peng, Y. Current status of optical fiber biosensor based on surface plasmon resonance. *Biosens. Bioelectron.* **2019**, *142*, 111505. [[CrossRef](#)] [[PubMed](#)]
12. Huang, J.; Zhou, Z.; Wen, X.; Zhang, D. A diaphragm-type fiber Bragg grating pressure sensor with temperature compensation. *Measurement* **2013**, *46*, 1041–1046. [[CrossRef](#)]
13. Sun, M.-Y.; Jiang, H.-T.; Shi, B.; Zhou, G.-Y.; Inyang, H.I.; Feng, C.-X. Development of FBG salinity sensor coated with lamellar polyimide and experimental study on salinity measurement of gravel aquifer. *Measurement* **2019**, *140*, 526–537. [[CrossRef](#)]
14. Erdody, S.; Korposh, S.; Lee, S.W.; Morgan, S.P. Long period grating fibre operating in visible range coated with porphyrin based thin film as an ammonia aqueous sensor. In Proceedings of the European Workshop on Optical Fibre Sensors (EWOFS 2023), Mons, Belgium, 23–26 May 2023; p. 126432R. [[CrossRef](#)]
15. Deleau, C.; Seat, H.C.; Surre, F.; Carcenac, F.; Calmon, P.-F.; Bernal, O. Gas Sensor Based on Silicon Nitride Integrated Long Period Grating. In Proceedings of the IEEE Sensors Conference, Dallas, TX, USA, 30 October–2 November 2022.
16. Saleh, A.; Mekhreguin, M.; Donsberg, T.; Kaariainen, T.; Genoud, G.; Toivonen, J. Mid-infrared hyperspectral sensor based on MEMS Fabry-Perot interferometer for stand-off sensing applications. *Sci. Rep.* **2022**, *12*, 19392. [[CrossRef](#)] [[PubMed](#)]
17. Li, H.; Bu, J.; Li, W.; Lv, J.; Wang, X.; Hu, K.; Yu, Y. Fiber optic Fabry-Perot sensor that can amplify ultrasonic wave for an enhanced partial discharge detection. *Sci. Rep.* **2021**, *11*, 8661. [[CrossRef](#)] [[PubMed](#)]
18. Dong, X.; Hu, P.; Chan, C.C.; Shum, P. Optical Fiber Humidity Sensor Based on Michelson Interferometric Structures. In Proceedings of the IEEE 6th International Conference on Advanced Infocomm Technology (ICAIT), Hsinchu, Taiwan, 6–9 July 2013; pp. 116–117.
19. Yuan, L.; Yang, J.; Liu, Z.; Sun, J. In-fiber integrated Michelson interferometer. *Opt. Lett.* **2006**, *31*, 2692–2694. [[CrossRef](#)] [[PubMed](#)]
20. Huang, X.; Li, X.; Yang, J.; Tao, C.; Guo, X.; Bao, H.; Yin, Y.; Chen, H.; Zhu, Y. An in-line Mach-Zehnder Interferometer Using Thin-core Fiber for Ammonia Gas Sensing with High Sensitivity. *Sci. Rep.* **2017**, *7*, 44994. [[CrossRef](#)]

21. Li, Y.; Wang, Y.; Wen, C. Temperature and strain sensing properties of the zinc coated FBG. *Optik* **2016**, *127*, 6463–6469. [[CrossRef](#)]
22. Wang, X.; Sun, X.; Hu, Y.; Zeng, L.; Liu, Q.; Duan, J.a. Highly-sensitive fiber Bragg grating temperature sensors with metallic coatings. *Optik* **2022**, *262*, 169337. [[CrossRef](#)]
23. Wang, J.N.; Zhou, X.L.; Miao, Y.F.; Jiang, G.C.; Tong, L.L.; Tao, P.C.; Yu, Q.X.; Peng, W. Integrated and compact fiber-optic conductivity-temperature-depth (CTD) sensor for marine detection. *Opt. Laser Technol.* **2023**, *164*, 109523. [[CrossRef](#)]
24. Urruti, E.H.; Wahl, J.F. Coatings affect fiber performance in smart-skin sensing. *Laser Focus World* **1990**, *26*, 169–170.
25. Orcel, G. Optical fiber coatings for sensing/smart skins applications. Fiber Optic Sensor-Based Smart Materials and Structures. In Proceedings of the Presented at the Fifth Annual Smart Materials and Structures Workshop, Blacksburg, Virginia, 15–16 April 1992; pp. 7–12.
26. Minghong, Y.; Chongjie, Q.; Jixiang, D.; Dongwen, L.; Jianguang, T. Optical fiber sensors with coatings as sensitive elements. In Proceedings of the Asia Communications and Photonics Conference, Shanghai, China, 11–14 November 2014; p. 3.
27. Liu, Y.; Jing, Z.; Liu, Q.; Li, A.; Lee, A.; Cheung, Y.; Zhang, Y.; Peng, W. All-silica fiber-optic temperature-depth-salinity sensor based on cascaded EFPIs and FBG for deep sea exploration. *Opt. Express* **2021**, *29*, 23953–23966. [[CrossRef](#)] [[PubMed](#)]
28. Massaroni, C.; Zaltieri, M.; Lo Presti, D.; Nicolo, A.; Tosi, D.; Schena, E. Fiber Bragg Grating Sensors for Cardiorespiratory Monitoring: A Review. *IEEE Sens. J.* **2021**, *21*, 14069–14080. [[CrossRef](#)]
29. Macheso, P.S.; Thulu, F.G.D. *Roles of Optical Fiber Sensors in the Internet of Things: Applications and Challenges*; Springer: Berlin/Heidelberg, Germany, 2023; pp. 923–933.
30. Cutolo, A.; Bernini, R.; Berruti, G.M.; Breglio, G.; Bruno, F.A.; Buontempo, S.; Catalano, E.; Consales, M.; Coscetta, A.; Cusano, A.; et al. Innovative Photonic Sensors for Safety and Security, Part II: Aerospace and Submarine Applications. *Sensors* **2023**, *23*, 2417. [[CrossRef](#)] [[PubMed](#)]
31. Zhang, P.; Zhang, X.Z.; Brown, J.; Vistisen, D.; Sicree, R.; Shaw, J.; Nichols, G. Global healthcare expenditure on diabetes for 2010 and 2030. *Diabetes Res. Clin. Pract.* **2010**, *87*, 293–301. [[CrossRef](#)] [[PubMed](#)]
32. Gerstein, H.C.; Beavers, D.P.; Bertoni, A.G.; Bigger, J.T.; Buse, J.B.; Craven, T.E.; Cushman, W.C.; Fonseca, V.; Geller, N.L.; Giddings, S.J.; et al. Nine-Year Effects of 3.7 Years of Intensive Glycemic Control on Cardiovascular Outcomes. *Diabetes Care* **2016**, *39*, 701–708. [[CrossRef](#)]
33. Zelnick, L.R.; Batacchi, Z.O.; Ahmad, I.; Dighe, A.; Little, R.R.; Trence, D.L.; Hirsch, I.B.; de Boer, I.H. Continuous Glucose Monitoring and Use of Alternative Markers To Assess Glycemia in Chronic Kidney Disease. *Diabetes Care* **2020**, *43*, 2379–2387. [[CrossRef](#)] [[PubMed](#)]
34. Nichols, S.P.; Koh, A.; Storm, W.L.; Shin, J.H.; Schoenfisch, M.H. Biocompatible Materials for Continuous Glucose Monitoring Devices. *Chem. Rev.* **2013**, *113*, 2528–2549. [[CrossRef](#)]
35. Levitt, D.L.; Silver, K.D.; Spanakis, E.K. Inpatient Continuous Glucose Monitoring and Glycemic Outcomes. *J. Diabetes Sci. Technol.* **2017**, *11*, 1028–1035. [[CrossRef](#)] [[PubMed](#)]
36. Oliver, N.S.; Toumazou, C.; Cass, A.E.G.; Johnston, D.G. Glucose sensors: A review of current and emerging technology. *Diabet. Med.* **2009**, *26*, 197–210. [[CrossRef](#)]
37. Pai, P.P.; Sanki, P.K.; Banerjee, S. A Photoacoustics based Continuous Non-Invasive Blood Glucose Monitoring System. In Proceedings of the 2015 IEEE International Symposium on Medical Measurements and Applications (MEMEA 2015) Proceedings, Politecnico Torino, Torino, Italy, 7–9 May 2015; pp. 106–111.
38. Sapozhnikova, V.V.; Kuranov, R.V.; Cicenaitė, I.; Esenaliev, R.O.; Prough, D.S. Effect on blood glucose monitoring of skin pressure exerted by an optical coherence tomography probe. *J. Biomed. Opt.* **2008**, *13*, 021112. [[CrossRef](#)]
39. He, Y.; Wang, X.; Sun, J.; Jiao, S.; Chen, H.; Gao, F.; Wang, L. Fluorescent blood glucose monitor by hemin-functionalized graphene quantum dots based sensing system. *Anal. Chim. Acta* **2014**, *810*, 71–78. [[CrossRef](#)]
40. Park, S.; Boo, H.; Chung, T.D. Electrochemical non-enzymatic glucose sensors. *Anal. Chim. Acta* **2006**, *556*, 46–57. [[CrossRef](#)]
41. Wilson, D.M.; Beck, R.W.; Tamborlane, W.V.; Dontchev, M.J.; Kollman, C.; Chase, P.; Fox, L.A.; Ruedy, K.J.; Tsalikian, E.; Weinzimer, S.A.; et al. The accuracy of the FreeStyle navigator continuous glucose monitoring system in children with type 1 diabetes. *Diabetes Care* **2007**, *30*, 59–64. [[CrossRef](#)]
42. Weinstein, R.L.; Bugler, J.R.; Schwartz, S.L.; Peyser, T.A.; Brazg, R.L.; McGarraugh, G.V. Accuracy of the 5-day freestyle navigator continuous glucose monitoring system—Comparison with frequent laboratory reference measurements. *Diabetes Care* **2007**, *30*, 1125–1130. [[CrossRef](#)] [[PubMed](#)]
43. Chen, G.; Wang, G.; Tan, X.; Hou, K.; Meng, Q.; Zhao, P.; Wang, S.; Zhang, J.; Zhou, Z.; Chen, T.; et al. Integrated dynamic wet spinning of core-sheath hydrogel fibers for optical-to-brain/tissue communications. *Natl. Sci. Rev.* **2021**, *8*, nwaa209. [[CrossRef](#)]
44. Chudnovskii, V.; Mayor, A.; Kiselev, A.; Yusupov, V. Foaming of blood in endovenous laser treatment. *Lasers Med. Sci.* **2018**, *33*, 1821–1826. [[CrossRef](#)] [[PubMed](#)]
45. Bian, S.; Shang, M.; Sawan, M. Rapid biosensing SARS-CoV-2 antibodies in vaccinated healthy donors. *Biosens. Bioelectron.* **2022**, *204*, 114054. [[CrossRef](#)] [[PubMed](#)]
46. Zhang, H.; Wang, K.; Li, W.T.; Ning, X.; Li, Y.R.; Qian, Z.Y. Design of blood flow imaging system based on fiber optic gastroscope. *Chin. Med. Equip. J.* **2020**, *41*, 13–17. [[CrossRef](#)]
47. Peterson, J.I.; Goldstein, S.R. A miniature fiberoptic pH sensor potentially suitable for glucose measurements. *Diabetes Care* **1982**, *5*, 272–274. [[CrossRef](#)]

48. Leonhardt, S.; Leonhardt. Portable Assembly to Detect and Correct Blood Sugar Level. DE19858426-A1; WO200103572-A1; DE19858426-C2; EP1194069-A1; US2002128543-A1; US6885881-B2; EP1194069-B1; DE59913262-G. Available online: <https://europepmc.org/article/PAT/DE19858426> (accessed on 25 January 2024).
49. Kuila, T.; Bose, S.; Khanra, P.; Mishra, A.K.; Kim, N.H.; Lee, J.H. Recent advances in graphene-based biosensors. *Biosens. Bioelectron.* **2011**, *26*, 4637–4648. [[CrossRef](#)]
50. Chen, D.; Feng, H.B.; Li, J.H. Graphene Oxide: Preparation, Functionalization, and Electrochemical Applications. *Chem. Rev.* **2012**, *112*, 6027–6053. [[CrossRef](#)]
51. Jiang, B.; Zhou, K.; Wang, C.; Sun, Q.; Yin, G.; Tai, Z.; Wilson, K.; Zhao, J.; Zhang, L. Label-free glucose biosensor based on enzymatic graphene oxide-functionalized tilted fiber grating. *Sens. Actuators B-Chem.* **2018**, *254*, 1033–1039. [[CrossRef](#)]
52. Panda, A.; Pukhrambam, P.D.; Keiser, G. Performance analysis of graphene-based surface plasmon resonance biosensor for blood glucose and gas detection. *Appl. Phys. A-Mater. Sci. Process.* **2020**, *126*, 153. [[CrossRef](#)]
53. Chen, X.Y.; Lin, W.W.; Xu, P.; Chen, L.X.; Meng, W.W.; Hu, X.H.; Qu, H.; Cui, Y.K.; Sun, J.H. FM-Level Detection of Glucose Using a Grating Based Sensor Enhanced With Graphene Oxide. *J. Light. Technol.* **2023**, *41*, 4145–4152. [[CrossRef](#)]
54. Mader, H.S.; Wolfbeis, O.S. Boronic acid based probes for microdetermination of saccharides and glycosylated biomolecules. *Microchim. Acta* **2008**, *162*, 1–34. [[CrossRef](#)]
55. Shiino, D.; Murata, Y.; Kataoka, K.; Koyama, Y.; Yokoyama, M.; Okano, T.; Sakurai, Y. Preparation and characterization of a glucose-responsive insulin-releasing polymer device. *Biomaterials* **1994**, *15*, 121–128. [[CrossRef](#)]
56. Samoei, G.K.; Wang, W.; Escobedo, J.O.; Xu, X.; Schneider, H.-J.; Cook, R.L.; Strongin, R.M. A chemomechanical polymer that functions in blood plasma with high glucose selectivity. *Angew. Chem.-Int. Ed.* **2006**, *45*, 5319–5322. [[CrossRef](#)] [[PubMed](#)]
57. Khan, M.R.R.; Watekar, A.V.; Kang, S.W. Fiber-Optic Biosensor to Detect pH and Glucose. *IEEE Sens. J.* **2018**, *18*, 1528–1538. [[CrossRef](#)]
58. Alexeev, V.L.; Sharma, A.C.; Goponenko, A.V.; Das, S.; Lednev, I.K.; Wilcox, C.S.; Finegold, D.N.; Asher, S.A. High ionic strength glucose-sensing photonic crystal. *Anal. Chem.* **2003**, *75*, 2316–2323. [[CrossRef](#)]
59. Li, Y.J.; Luo, S.T.; Gui, Y.Q.; Wang, X.; Tian, Z.Y.; Yu, H.H. Difunctional Hydrogel Optical Fiber Fluorescence Sensor for Continuous and Simultaneous Monitoring of Glucose and pH. *Biosensors* **2023**, *13*, 287. [[CrossRef](#)]
60. Sridevi, S.; Vasu, K.S.; Sampath, S.; Asokan, S.; Sood, A.K. Optical detection of glucose and glycated hemoglobin using etched fiber Bragg gratings coated with functionalized reduced graphene oxide. *J. Biophotonics* **2016**, *9*, 760–769. [[CrossRef](#)]
61. Tao, M.; Jin, Y.; Gu, N.; Huang, L. A method to control the fabrication of etched optical fiber probes with nanometric tips. *J. Opt.* **2010**, *12*, 015503. [[CrossRef](#)]
62. Koo, K.N.; Ismail, A.F.; Othman, M.H.D.; Tai, Z.S.; Abu Bakar, M.A.; Rahman, M.A.; Samavati, A. Tailoring surface structure and diameter of etched fiber Bragg grating for high strain sensing. *Opt. Laser Technol.* **2023**, *157*, 108693. [[CrossRef](#)]
63. Mohamed, M.S.; Hameed, M.F.O.; Areed, N.F.F.; El-Okri, M.M.; Obayya, S.S.A. Analysis of Highly Sensitive Photonic Crystal Biosensor for Glucose Monitoring. *Appl. Comput. Electromagn. Soc. J.* **2016**, *31*, 836–842.
64. Li, X.G.; Gong, P.Q.; Zhang, Y.A.; Zhou, X. Label-Free Micro Probe Optical Fiber Biosensor for Selective and Highly Sensitive Glucose Detection. *IEEE Trans. Instrum. Meas.* **2022**, *71*, 7008608. [[CrossRef](#)]
65. Cunha, C.; Assunção, A.S.; Monteiro, C.S.; Leitao, C.; Mendes, J.P.; Silva, S.; Frazao, O.; Novais, S. Transmissive glucose concentration plasmonic Au sensor based on unclad optical fiber. In Proceedings of the IEEE 7th Portuguese Meeting on Bioengineering (ENBENG), Porto, Portugal, 22–23 June 2023; pp. 13–16.
66. Li, Y.P.; Ma, H.; Gan, L.; Liu, Q.; Yan, Z.J.; Liu, D.M.; Sun, Q.Z. Immobilized optical fiber microprobe for selective and high sensitive glucose detection. *Sens. Actuators B-Chem.* **2018**, *255*, 3004–3010. [[CrossRef](#)]
67. Zhang, X.; Zhang, J.; Zhang, F.; Yu, S. Probing the binding affinity of plasma proteins adsorbed on Au nanoparticles. *Nanoscale* **2017**, *9*, 4787–4792. [[CrossRef](#)] [[PubMed](#)]
68. Li, D.C.; Yu, S.L.; Sun, C.Y.; Zou, C.W.; Yu, H.X.; Xu, K.X. U-shaped fiber-optic ATR sensor enhanced by silver nanoparticles for continuous glucose monitoring. *Biosens. Bioelectron.* **2015**, *72*, 370–375. [[CrossRef](#)]
69. Yin, M.J.; Huang, B.B.; Gao, S.R.; Zhang, A.P.; Ye, X.S. Optical fiber LPG biosensor integrated microfluidic chip for ultrasensitive glucose detection. *Biomed. Opt. Express* **2016**, *7*, 2067–2077. [[CrossRef](#)] [[PubMed](#)]
70. Johnson, P.B.; Christy, R.W. Optical constants of the noble metals. *Phys. Rev. B (Solid State)* **1972**, *6*, 4370–4379. [[CrossRef](#)]
71. Frost, M.C.; Meyerhoff, M.E. Real-Time Monitoring of Critical Care Analytes in the Bloodstream with Chemical Sensors: Progress and Challenges. *Annu. Rev. Anal. Chem.* **2015**, *8*, 171–192. [[CrossRef](#)]
72. Liu, R.; Liu, L.; Liang, J.; Wang, Y.; Wei, Y.; Gao, F.; Gao, L.; Gao, X. Detection of pH Change in Cytoplasm of Live Myocardial Ischemia Cells via the ssDNA-SWCNTs Nanoprobes. *Anal. Chem.* **2014**, *86*, 3048–3052. [[CrossRef](#)]
73. Ma, W.; Yan, L.a.; He, X.; Qing, T.; Lei, Y.; Qiao, Z.; He, D.; Huang, K.; Wang, K. Hairpin-Contained i-Motif Based Fluorescent Ratiometric Probe for High-Resolution and Sensitive Response of Small pH Variations. *Anal. Chem.* **2018**, *90*, 1889–1896. [[CrossRef](#)]
74. Wang, J.; Geng, Y.; Shen, Y.; Shi, W.; Xu, W.; Xu, S. SERS-active fiber tip for intracellular and extracellular pH sensing in living single cells. *Sens. Actuators B-Chem.* **2019**, *290*, 527–534. [[CrossRef](#)]
75. Chesler, M. Regulation and modulation of pH in the brain. *Physiol. Rev.* **2003**, *83*, 1183–1221. [[CrossRef](#)]
76. Pullano, S.A.; Critello, C.D.; Mahbub, I.; Tasneem, N.T.; Shamsir, S.; Islam, S.K.; Greco, M.; Fiorillo, A.S. EGFET-Based Sensors for Bioanalytical Applications: A Review. *Sensors* **2018**, *18*, 4042. [[CrossRef](#)]

77. Vivaldi, F.; Santalucia, D.; Poma, N.; Bonini, A.; Salvo, P.; Del Noce, L.; Melai, B.; Kirchhain, A.; Kolivoska, V.; Sokolova, R.; et al. A voltammetric pH sensor for food and biological matrices (vol 322, 128650, 2020). *Sens. Actuators B-Chem.* **2021**, *330*, 129176. [[CrossRef](#)]
78. Pastore, A.; Badocco, D.; Pastore, P. Reversible and high accuracy pH colorimetric sensor array based on a single acid-base indicator working in a wide pH interval. *Talanta* **2020**, *219*, 121251. [[CrossRef](#)]
79. Huang, J.; Ying, L.; Yang, X.; Yang, Y.; Quan, K.; Wang, H.; Xie, N.; Ou, M.; Zhou, Q.; Wang, K. Ratiometric Fluorescent Sensing of pH Values in Living Cells by Dual-Fluorophore-Labeled i-Motif Nanoprobes. *Anal. Chem.* **2015**, *87*, 8724–8731. [[CrossRef](#)]
80. Wencel, D.; Kaworek, A.; Abel, T.; Efremov, V.; Bradford, A.; Carthy, D.; Coady, G.; McMorro, R.C.N.; McDonagh, C. Optical Sensor for Real-Time pH Monitoring in Human Tissue. *Small* **2018**, *14*, 1803627. [[CrossRef](#)]
81. Baldini, F.; Mignani, A.G. Optical-fiber medical sensors. *Mrs Bull.* **2002**, *27*, 383–387. [[CrossRef](#)]
82. Aigner, D.; Ungerboeck, B.; Mayr, T.; Saf, R.; Klimant, I.; Borisov, S.M. Fluorescent materials for pH sensing and imaging based on novel 1,4-diketopyrrolo-3,4-c pyrrole dyes. *J. Mater. Chem. C* **2013**, *1*, 5685–5693. [[CrossRef](#)]
83. Richter, A.; Paschew, G.; Klatt, S.; Lienig, J.; Arndt, K.-F.; Adler, H.-J.P. Review on hydrogel-based pH sensors and microsensors. *Sensors* **2008**, *8*, 561–581. [[CrossRef](#)]
84. Asare, K.P.; Zniber, M.; Zouheir, M.; Wang, L.; Wang, X.; Tan-Phat, H. Luciferin-based fluorescent hydrogel as a pH sensor. *Mrs Commun.* **2022**, *12*, 90–94. [[CrossRef](#)]
85. Skorjanc, T.; Shetty, D.; Valant, M. Covalent Organic Polymers and Frameworks for Fluorescence-Based Sensors. *Acs Sens.* **2021**, *6*, 1461–1481. [[CrossRef](#)]
86. Mohammadnia, M.S.; Roghani-Mamaqani, H.; Mardani, H.; Rezvani-Moghaddam, A.; Hemmati, S.; Salami-Kalajahi, M. Fluorescent cellulosic composites based on carbon dots: Recent advances, developments, and applications. *Carbohydr. Polym.* **2022**, *294*, 119768. [[CrossRef](#)]
87. Di Costanzo, L.; Panunzi, B. Visual pH Sensors: From a Chemical Perspective to New Bioengineered Materials. *Molecules* **2021**, *26*, 2952. [[CrossRef](#)]
88. Yetisen, A.K.; Jiang, N.; Fallahi, A.; Montelongo, Y.; Ruiz-Esparza, G.U.; Tamayol, A.; Zhang, Y.S.; Mahmood, I.; Yang, S.-A.; Kim, K.S.; et al. Glucose-Sensitive Hydrogel Optical Fibers Functionalized with Phenylboronic Acid. *Adv. Mater.* **2017**, *29*, 1606380. [[CrossRef](#)]
89. Elsherif, M.; Salih, A.E.; Muñoz, M.G.; Alam, F.; AlQattan, B.; Antonysamy, D.S.; Zaki, M.F.; Yetisen, A.K.; Park, S.; Wilkinson, T.D.; et al. Optical Fiber Sensors: Working Principle, Applications, and Limitations. *Adv. Photonics Res.* **2022**, *3*, 2100371. [[CrossRef](#)]
90. Peterson, J.I.; Goldstein, S.R.; Fitzgerald, R.V.; Buckhold, D.K. Fiber optic pH probe for physiological use. *Anal. Chem.* **1980**, *52*, 864–869. [[CrossRef](#)]
91. Jin, W.; Wu, L.; Song, Y.; Jiang, J.; Zhu, X.; Yang, D.; Bai, C. Continuous Intra-Arterial Blood pH Monitoring by a Fiber-Optic Fluorosensor. *IEEE Trans. Biomed. Eng.* **2011**, *58*, 1232–1238. [[CrossRef](#)]
92. Levy, R.; Guignon, E.F.; Cobane, S.; St. Louis, E.; Fernandez, S.M. Compact, rugged and inexpensive frequency-domain fluorometer. *Proc. SPIE-Int. Soc. Opt. Eng.* **1997**, *2980*, 81–89. [[CrossRef](#)]
93. Ehrlich, K.; Kufcsak, A.; Krstajic, N.; Henderson, R.K.; Thomson, R.R.; Tanner, M.G. Fibre optic time-resolved spectroscopy using CMOS-SPAD arrays. In Proceedings of the Conference on Optical Fibers and Sensors for Medical Diagnostics and Treatment Applications XVII, San Francisco, CA, USA, 28–29 January 2017.
94. Podrazky, O.; Mrázek, J.; Probstová, J.; Vytýkáčová, S.; Kasík, I.; Pitrová, S.; Jasim, A.A. Ex-Vivo Measurement of the pH in Aqueous Humor Samples by a Tapered Fiber-Optic Sensor. *Sensors* **2021**, *21*, 5075. [[CrossRef](#)]
95. Zhao, Q.; Yin, M.; Zhang, A.P.; Prescher, S.; Antonietti, M.; Yuan, J. Hierarchically Structured Nanoporous Poly(Ionic Liquid) Membranes: Facile Preparation and Application in Fiber-Optic pH Sensing. *J. Am. Chem. Soc.* **2013**, *135*, 5549–5552. [[CrossRef](#)]
96. Zhao, Q.; Dunlop, J.W.C.; Qiu, X.; Huang, F.; Zhang, Z.; Heyda, J.; Dzubiella, J.; Antonietti, M.; Yuan, J. An instant multi-responsive porous polymer actuator driven by solvent molecule sorption. *Nat. Commun.* **2014**, *5*, 4293. [[CrossRef](#)]
97. Zhao, C.; Nie, S.; Tang, M.; Sun, S. Polymeric pH-sensitive membranes-A review. *Prog. Polym. Sci.* **2011**, *36*, 1499–1520. [[CrossRef](#)]
98. Chiang, E.N.; Dong, R.; Ober, C.K.; Baird, B.A. Cellular Responses to Patterned Poly(acrylic acid) Brushes. *Langmuir* **2011**, *27*, 7016–7023. [[CrossRef](#)]
99. Yin, M.-J.; Yao, M.; Gao, S.; Zhang, A.P.; Tam, H.-Y.; Wai, P.-K.A. Rapid 3D Patterning of Poly(acrylic acid) Ionic Hydrogel for Miniature pH Sensors. *Adv. Mater.* **2016**, *28*, 1394–1399. [[CrossRef](#)]
100. Gu, B.; Yin, M.; Zhang, A.P.; Qian, J.; He, S. Biocompatible Fiber-Optic pH Sensor Based on Optical Fiber Modal Interferometer Self-Assembled With Sodium Alginate/Polyethylenimine Coating. *IEEE Sens. J.* **2012**, *12*, 1477–1482. [[CrossRef](#)]
101. Lopez Aldabaa, A.; Gonzalez-Vila, A.; Debliquy, M.; Lopez-Amo, M.; Caucheteur, C.; Lahem, D. Polyaniline-coated tilted fiber Bragg gratings for pH sensing. *Sens. Actuators B-Chem.* **2018**, *254*, 1087–1093. [[CrossRef](#)]
102. Mishra, S.K.; Zou, B.; Chiang, K.S. Wide-Range pH Sensor Based on a Smart-Hydrogel-Coated Long-Period Fiber Grating. *IEEE J. Sel. Top. Quantum Electron.* **2017**, *23*, 5601405. [[CrossRef](#)]
103. Zhao, Y.; Lei, M.; Liu, S.-X.; Zhao, Q. Smart hydrogel-based optical fiber SPR sensor for pH measurements. *Sens. Actuators B-Chem.* **2018**, *261*, 226–232. [[CrossRef](#)]
104. Humpolicek, P.; Kasparkova, V.; Saha, P.; Stejskal, J. Biocompatibility of polyaniline. *Synth. Met.* **2012**, *162*, 722–727. [[CrossRef](#)]
105. Chiam, Y.S.; Ahad, I.Z.M.; Harun, S.W.; Gan, S.N.; Phang, S.W. Effects of the Dopant Ratio on Polyaniline Coated Fiber Bragg Grating for pH detection. *Synth. Met.* **2016**, *211*, 132–141. [[CrossRef](#)]

106. Massaroni, C.; Saccomandi, P.; Schena, E. Medical Smart Textiles Based on Fiber Optic Technology: An Overview. *J. Funct. Biomater.* **2015**, *6*, 204–221. [CrossRef]
107. Witt, J.; Narbonneau, F.; Schukar, M.; Krebber, K.; De Jonckheere, J.; Jeanne, M.; Kinet, D.; Paquet, B.; Depre, A.; D'Angelo, L.T.; et al. Medical Textiles With Embedded Fiber Optic Sensors for Monitoring of Respiratory Movement. *IEEE Sens. J.* **2012**, *12*, 246–254. [CrossRef]
108. Mishra, V.; Singh, N.; Tiwari, U.; Kapur, P. Fiber grating sensors in medicine: Current and emerging applications. *Sens. Actuators A-Phys.* **2011**, *167*, 279–290. [CrossRef]
109. Wang, Y.J.; Zhang, H.; Cui, Y.X.; Duan, S.X.; Lin, W.; Liu, B. A complementary-DNA-enhanced fiber-optic sensor based on microfiber-assisted Mach-Zehnder interferometry for biocompatible pH sensing. *Sens. Actuators B-Chem.* **2021**, *332*, 129516. [CrossRef]
110. Mani, G.K.; Miyakoda, K.; Saito, A.; Yasoda, Y.; Kajiwara, K.; Kimura, M.; Tsuchiya, K. Microneedle pH Sensor: Direct, Label-Free, Real-Time Detection of Cerebrospinal Fluid and Bladder pH. *Acs Appl. Mater. Interfaces* **2017**, *9*, 21651–21659. [CrossRef]
111. Siesjo, B.K. Symposium on acid-base homeostasis. The regulation of cerebrospinal fluid pH. *Kidney Int.* **1972**, *1*, 360–374. [CrossRef]
112. Shi, W.; Li, X.; Ma, H. A Tunable Ratiometric pH Sensor Based on Carbon Nanodots for the Quantitative Measurement of the Intracellular pH of Whole Cells. *Angew. Chem.-Int. Ed.* **2012**, *51*, 6432–6435. [CrossRef]
113. Zhou, B.Q.; Fan, K.K.; Li, T.F.; Luan, G.M.; Kong, L.J. A biocompatible hydrogel-coated fiber-optic probe for monitoring pH dynamics in mammalian brains in vivo. *Sens. Actuators B-Chem.* **2023**, *380*, 133334. [CrossRef]
114. Steinegger, A.; Wolfbeis, O.S.; Borisov, S.M. Optical Sensing and Imaging of pH Values: Spectroscopies, Materials, and Applications. *Chem. Rev.* **2020**, *120*, 12357–12489. [CrossRef]
115. lesonco. Available online: <https://www.lesonco.com/index.php/2019-11-19-09-34-23/item/28-ph> (accessed on 24 January 2024).
116. Medical EXPO. Available online: <https://www.medicalex-po.com.cn/prod/tecnovet/product-124655-1093032.html> (accessed on 24 January 2024).
117. PreSens. Available online: <https://presens.com.cn/product/ph/sensor/261#c1254> (accessed on 24 January 2024).
118. ANALOG DEVOCES. Available online: <https://www.analog.com/cn/technical-articles/ph-sensor-reference-design-enabled-for-rf-wireless-transmission.html> (accessed on 24 January 2024).
119. Liu, J.T.; Chen, C.J.; Ikoma, T.; Yoshioka, T.; Cross, J.S.; Chang, S.-J.; Tsai, J.-Z.; Tanaka, J. Surface plasmon resonance biosensor with high anti-fouling ability for the detection of cardiac marker troponin T. *Anal. Chim. Acta* **2011**, *703*, 80–86. [CrossRef]
120. Ishani, A.; Grandits, G.A.; Grimm, R.H.; Svendsen, K.H.; Collins, A.J.; Prineas, R.J.; Neaton, J.D.; Grp, M.R. Association of single measurements of dipstick proteinuria, estimated glomerular filtration rate, and hematocrit with 25-year incidence of end-stage renal disease in the multiple risk factor intervention trial. *J. Am. Soc. Nephrol.* **2006**, *17*, 1444–1452. [CrossRef]
121. Tonelli, M.; Muntner, P.; Lloyd, A.; Manns, B.J.; James, M.T.; Klarenbach, S.; Quinn, R.R.; Wiebe, N.; Hemmelgarn, B.R.; Alberta Kidney Dis, N. Using Proteinuria and Estimated Glomerular Filtration Rate to Classify Risk in Patients with Chronic Kidney Disease A Cohort Study. *Ann. Intern. Med.* **2011**, *154*, 12-U146. [CrossRef]
122. Agrawal, V.; Marinescu, V.; Agarwal, M.; McCullough, P.A. Cardiovascular implications of proteinuria: An indicator of chronic kidney disease. *Nat. Rev. Cardiol.* **2009**, *6*, 301–311. [CrossRef]
123. Guo, T.; Liu, F.; Liang, X.; Qiu, X.H.; Huang, Y.Y.; Xie, C.; Xu, P.; Mao, W.; Guan, B.O.; Albert, J. Highly sensitive detection of urinary protein variations using tilted fiber grating sensors with plasmonic nanocoatings. *Biosens. Bioelectron.* **2016**, *78*, 221–228. [CrossRef]
124. Dennis, J.W.; Granovsky, M.; Warren, C.E. Protein glycosylation in development and disease. *Bioessays* **1999**, *21*, 412–421. [CrossRef]
125. Santos, A.; Bueno, P.R. Glycoprotein assay based on the optimized immittance signal of a redox tagged and lectin-based receptive interface. *Biosens. Bioelectron.* **2016**, *83*, 368–378. [CrossRef]
126. Fang, W.; Yang, Z.; Zigeng, L.; Siyu, Q.; Yiyang, G.; Zhenguang, J.; Changsen, S.; Wei, P. Detection of Glycoprotein using fiber optic surface plasmon resonance sensors with Boronic acid. In Proceedings of the 2017 25th Optical Fiber Sensors Conference (OFS), Jeju, Republic of Korea, 24–28 April 2017; p. 103233W. [CrossRef]
127. Fu, F.; Dong, H.; Song, C. Clinical significance of myocardial injury index and inflammatory index in patients with acute myocardial infarction. *Chin. J. Clin. Lab. Manag. (Electron. Ed.)* **2021**, *9*, 160–163.
128. Tomyshev, K.A.; Tazhetdinova, D.K.; Butov, O.V. High-resolution Fiber Plasmon Sensor. In Proceedings of the Progress in Electromagnetics Research Symposium—Spring (PIERS), St. Petersburg, Russia, 22–25 May 2017; pp. 53–56.
129. Kanapathipillai, M. Treating p53 Mutant Aggregation-Associated Cancer. *Cancers* **2018**, *10*, 154. [CrossRef]
130. McGrath, E.P.; Logue, S.E.; Mnich, K.; Deegan, S.; Jaeger, R.; Gorman, A.M.; Samali, A. The Unfolded Protein Response in Breast Cancer. *Cancers* **2018**, *10*, 344. [CrossRef]
131. Groh, N.; Buehler, A.; Huang, C.; Li, K.W.; van Nierop, P.; Smit, A.B.; Faendrich, M.; Baumann, F.; David, D.C. Age-Dependent Protein Aggregation Initiates Amyloid- β Aggregation. *Front. Aging Neurosci.* **2017**, *9*, 138. [CrossRef]
132. Goedert, M.; Spillantini, M.G.; Cairns, N.J.; Crowther, R.A. Tau proteins of Alzheimer paired helical filaments: Abnormal phosphorylation of all six brain isoforms. *Neuron* **1992**, *8*, 159–168. [CrossRef]

133. Iqbal, K.; Alonso, A.D.C.; Chen, S.; Chohan, M.O.; El-Akkad, E.; Gong, C.X.; Khatoon, S.; Li, B.; Liu, F.; Rahman, A.; et al. Tau pathology in Alzheimer disease and other tauopathies. *Biochim. Biophys. Acta-Mol. Basis Dis.* **2005**, *1739*, 198–210. [[CrossRef](#)]
134. Fatima Domingues, M.; Direito, I.; Sousa, C.; Radwan, A.; Antunes, P.; Andre, P.; Helguero, L.; Alberto, N. Optical Fibre FPI End-Tip based Sensor for Protein Aggregation Detection. In Proceedings of the 2022 IEEE International Conference on E-health Networking, Application & Services (HealthCom), Genoa, Italy, 17–19 October 2022; pp. 129–134. [[CrossRef](#)]
135. Nu, T.T.V.; Tran, N.H.T.; Nam, E.; Nguyen, T.T.; Yoon, W.J.; Cho, S.; Kim, J.; Chang, K.A.; Ju, H. Blood-based immunoassay of tau proteins for early diagnosis of Alzheimer’s disease using surface plasmon resonance fiber sensors. *Rsc Adv.* **2018**, *8*, 7855–7862. [[CrossRef](#)]
136. Papadea, C.; Check, I.J. Human immunoglobulin G and immunoglobulin G subclasses: Biochemical, genetic, and clinical aspects. *Crit. Rev. Clin. Lab. Sci.* **1989**, *27*, 27–58. [[CrossRef](#)]
137. Soderstrom, T.; Soderstrom, R.; Enskog, A. Immunoglobulin subclasses and prophylactic use of immunoglobulin in immunoglobulin G subclass deficiency. *Cancer* **1991**, *68*, 1426–1429. [[CrossRef](#)] [[PubMed](#)]
138. Wang, Q.; Jing, J.Y.; Wang, B.T. Highly Sensitive SPR Biosensor Based on Graphene Oxide and Staphylococcal Protein A Co-Modified TFBG for Human IgG Detection. *IEEE Trans. Instrum. Meas.* **2019**, *68*, 3350–3357. [[CrossRef](#)]
139. Chen, S.M.; Zhang, C.; Wang, J.H.; Li, N.; Song, Y.X.; Wu, H.J.; Liu, Y. A Fiber Bragg Grating Sensor Based on Cladding Mode Resonance for Label-Free Biosensing. *Biosensors* **2023**, *13*, 97. [[CrossRef](#)] [[PubMed](#)]
140. Kamil, Y.M.; Abu Bakar, M.H.; Yaacob, M.H.; Syahir, A.; Lim, H.N.; Mahdi, M.A. Dengue E Protein Detection Using a Graphene Oxide Integrated Tapered Optical Fiber Sensor. *IEEE J. Sel. Top. Quantum Electron.* **2019**, *25*, 7201008. [[CrossRef](#)]
141. Dhara, K.; Mahapatra, D.R. Review on electrochemical sensing strategies for C-reactive protein and cardiac troponin I detection. *Microchem. J.* **2020**, *156*, 104857. [[CrossRef](#)]
142. Abdolrahim, M.; Rabiee, M.; Alhosseini, S.N.; Tahriri, M.; Yazdanpanah, S.; Tayebi, L. Development of optical biosensor technologies for cardiac troponin recognition. *Anal. Biochem.* **2015**, *485*, 1–10. [[CrossRef](#)] [[PubMed](#)]
143. Dhawan, S.; Sadanandan, S.; Haridas, V.; Voelcker, N.H.; Prieto-Simon, B. Novel peptidylated surfaces for interference-free electrochemical detection of cardiac troponin I. *Biosens. Bioelectron.* **2018**, *99*, 486–492. [[CrossRef](#)] [[PubMed](#)]
144. Wang, Y.; Singh, R.; Li, M.Y.; Min, R.; Wu, Q.; Kaushik, B.K.; Jha, R.; Zhang, B.Y.; Kumar, S. Cardiac Troponin I Detection Using Gold/Cerium-Oxide Nanoparticles Assisted Hetro-Core Fiber Structure. *IEEE Trans. Nanobioscience* **2023**, *22*, 375–382. [[CrossRef](#)]
145. Li, B.; Zhao, M.; Feng, L.; Dou, C.; Ding, S.; Zhou, G.; Lu, L.; Zhang, H.; Chen, F.; Li, X.; et al. Organic NIR-II molecule with long blood half-life for in vivo dynamic vascular imaging. *Nat. Commun.* **2020**, *11*, 3102. [[CrossRef](#)]
146. Benndorf, G.; Singel, S.; Proest, G.; Lanksch, W.; Felix, R. The Doppler guide wire: Clinical applications in neuroendovascular treatment. *Neuroradiology* **1997**, *39*, 286–291. [[CrossRef](#)]
147. Benndorf, G.; Wellnhofer, E.; Lanksch, W.; Felix, R. Intraaneurysmal flow: Evaluation with Doppler guidewires. *Ajnr* **1996**, *17*, 1333–1337.
148. Hsu, B. PET tracers and techniques for measuring myocardial blood flow in patients with coronary artery disease. *J. Biomed. Res.* **2013**, *27*, 452–459. [[CrossRef](#)]
149. Ruiz-Vargas, A.; Morris, S.A.; Hartley, R.H.; Arkwright, J.W. Optical flow sensor for continuous invasive measurement of blood flow velocity. *J. Biophotonics* **2019**, *12*, e201900139. [[CrossRef](#)]
150. Tanaka, T.; Benedek, G.B. Measurement of the Velocity of Blood Flow (in vivo) Using a Fiber Optic Catheter and Optical Mixing Spectroscopy. *Appl. Opt.* **1975**, *14*, 189–196. [[CrossRef](#)]
151. Wu, Y.C. Design of Portable Body Rheometer. *J. Xi’an Aeronaut. Inst.* **2011**, *29*, 61–63.
152. Tahmoush, A.J.; Bowen, P.D.; Bonner, R.F.; Mancini, T.J.; Engel, W.K. Laser Doppler blood flow studies during open muscle biopsy in patients with neuromuscular diseases. *Neurology* **1983**, *33*, 547–551. [[CrossRef](#)] [[PubMed](#)]
153. Peterson, J.I.; Vurek, G.G. Fiber-optic sensors for biomedical applications. *Science* **1984**, *224*, 123–127. [[CrossRef](#)] [[PubMed](#)]
154. Le-Cong, P.; Zweifach, B.W. In vivo and in vitro velocity measurements in microvasculature with a laser. *Microvasc. Res.* **1979**, *17*, 131–141. [[CrossRef](#)] [[PubMed](#)]
155. Gattinoni, L.; Agostoni, A.; Pesenti, A.; Pelizzola, A.; Rossi, G.P.; Langer, M.; Vesconi, S.; Uziel, L.; Fox, U.; Longoni, F.; et al. Treatment of acute respiratory failure with low-frequency positive-pressure ventilation and extracorporeal removal of CO₂. *Lancet* **1980**, *2*, 292–294. [[CrossRef](#)] [[PubMed](#)]
156. Damianou, D. The Wavelength Dependence of the Photoplethysmogram and Its Implication to Pulse Oximetry. Ph.D. Thesis, University of Nottingham, Nottingham, UK, 1995.
157. Reichelt, S.; Fiala, J.; Werber, A.; Foerster, K.; Heilmann, C.; Klemm, R.; Zappe, H. Development of an implantable pulse oximeter. *IEEE Trans. Biomed. Eng.* **2008**, *55*, 581–588. [[CrossRef](#)] [[PubMed](#)]
158. Liu, C.; Correia, R.; Ballaji, H.K.; Korposh, S.; Hayes-Gill, B.R.; Morgan, S.P. Optical Fibre-Based Pulse Oximetry Sensor with Contact Force Detection. *Sensors* **2018**, *18*, 3632. [[CrossRef](#)] [[PubMed](#)]
159. Chen, C.Y.; Wang, W.K.; Kao, T.; Yu, B.C.; Chiang, B.C. Spectral analysis of radial pulse in patients with acute, uncomplicated myocardial infarction. *Jpn. Heart J.* **1993**, *34*, 131–143. [[CrossRef](#)]
160. Yu, G.L.; Wang, Y.Y.L.; Wang, W.K. Resonance in the kidney system of rats. *Am. J. Physiol.* **1994**, *267*, H1544–H1548. [[CrossRef](#)]
161. Lu, W.A.; Cheng, C.H.; Wang, Y.Y.L.; Wang, W.K. Pulse spectrum analysis of hospital patients with possible liver problems. *Am. J. Chin. Med.* **1996**, *24*, 315–320. [[CrossRef](#)]

162. Pauca, A.L.; O'Rourke, M.F.; Kon, N.D. Prospective evaluation of a method for estimating ascending aortic pressure from the radial artery pressure waveform. *Hypertension* **2001**, *38*, 932–937. [[CrossRef](#)]
163. Nichols, W.W.; Singh, B.M. Augmentation index as a measure of peripheral vascular disease state. *Curr. Opin. Cardiol.* **2002**, *17*, 543–551. [[CrossRef](#)]
164. Otsuka, T.; Munakata, R.; Kato, K.; Kodani, E.; Ibuki, C.; Kusama, Y.; Seino, Y.; Kawada, T. Oscillometric measurement of brachial artery cross-sectional area and its relationship with cardiovascular risk factors and arterial stiffness in a middle-aged male population. *Hypertens. Res.* **2013**, *36*, 910–915. [[CrossRef](#)]
165. Haseda, Y.; Bonefacino, J.; Tam, H.Y.; Chino, S.; Koyama, S.; Ishizawa, H. Measurement of Pulse Wave Signals and Blood Pressure by a Plastic Optical Fiber FBG Sensor. *Sensors* **2019**, *19*, 5088. [[CrossRef](#)] [[PubMed](#)]
166. Pant, S.; Umesh, S.; Asokan, S. A Novel Approach to Acquire the Arterial Pulse by Finger Plethysmography Using Fiber Bragg Grating Sensor. *IEEE Sens. J.* **2020**, *20*, 5921–5928. [[CrossRef](#)]
167. Lukman, S.; He, Y.; Hui, S.-C. Computational methods for Traditional Chinese Medicine: A survey. *Comput. Methods Programs Biomed.* **2007**, *88*, 283–294. [[CrossRef](#)] [[PubMed](#)]
168. Jeon, Y.J.; Kim, J.U.; Lee, H.J.; Lee, J.; Ryu, H.H.; Lee, Y.J.; Kim, J.Y. A Clinical Study of the Pulse Wave Characteristics at the Three Pulse Diagnosis Positions of Chon, Gwan and Cheok. *Evid.-Based Complement. Altern. Med.* **2011**, *2011*, 904056. [[CrossRef](#)] [[PubMed](#)]
169. Shu, J.-J.; Sun, Y. Developing classification indices for Chinese pulse diagnosis. *Complement. Ther. Med.* **2007**, *15*, 190–198. [[CrossRef](#)] [[PubMed](#)]
170. Gong, J.; Lu, S.; Wang, R.; Cui, L. PDhms: Pulse Diagnosis via Wearable Healthcare Sensor Network. In Proceedings of the 2011 IEEE International Conference on Communications (ICC), Kyoto, Japan, 5–9 June 2011; 2011; p. 5.
171. Jia, D.G.; Chao, J.; Li, S.; Zhang, H.X.; Yan, Y.Z.; Liu, T.G.; Sun, Y. A Fiber Bragg Grating Sensor for Radial Artery Pulse Waveform Measurement. *IEEE Trans. Biomed. Eng.* **2018**, *65*, 839–846. [[CrossRef](#)]
172. Koyama, S.; Hayase, T.; Miyauchi, S.; Shirai, A.; Chino, S.; Haseda, Y.; Ishizawa, H. Influence on Measurement Signal by Pressure and Viscosity Changes of Fluid and Installation Condition of FBG Sensor Using Blood Flow Simulation Model. *IEEE Sens. J.* **2019**, *19*, 11946–11954. [[CrossRef](#)]
173. Ghasemi, M.; Oh, J.; Jeong, S.; Lee, M.; Darian, S.B.; Oh, K.; Kim, J.K. Fabry-Perot Interferometric Fiber-Optic Sensor for Rapid and Accurate Thrombus Detection. *Biosensors* **2023**, *13*, 817. [[CrossRef](#)] [[PubMed](#)]

Disclaimer/Publisher's Note: The statements, opinions and data contained in all publications are solely those of the individual author(s) and contributor(s) and not of MDPI and/or the editor(s). MDPI and/or the editor(s) disclaim responsibility for any injury to people or property resulting from any ideas, methods, instructions or products referred to in the content.